

New results from nuclear lattice simulations

Dean Lee
Facility for Rare Isotope Beams
Michigan State University
Nuclear Lattice EFT Collaboration

Workshop on Progress in Ab Initio Nuclear Theory
TRIUMF
February 26, 2026



arXiv:2602.17611

Evidence for Multimodal Superfluidity of Neutrons

**Yuan-Zhuo Ma^{1,2}, Georgios Palkanoglou^{3,4}, Joseph Carlson⁵, Stefano Gandolfi⁵,
Alexandros Gezerlis⁴, Gabriel Given^{1,2}, Ashe Hicks^{1,2}, Dean Lee^{1,2}, Kevin E. Schmidt⁶, and
Jiabin Yu⁷**

¹Facility for Rare Isotope Beams, Michigan State University, East Lansing, Michigan 48824

²Department of Physics and Astronomy, Michigan State University, East Lansing, Michigan 48824

³TRIUMF, 4004 Wesbrook Mall, Vancouver, BC V6T 2A3, Canada

⁴Department of Physics, University of Guelph, Guelph, ON N1G 2W1, Canada

⁵Theoretical Division, Los Alamos National Laboratory, Los Alamos, NM 87545, USA

⁶Department of Physics, Arizona State University, Tempe, Arizona 85287, USA

⁷Department of Physics and Quantum Theory Project, University of Florida, Gainesville, FL 32611, USA

Outline

Lattice effective field theory

Superfluid condensation

Wavefunction matching

Unitary limit

Generalized attractive
extended Hubbard model

Multimodal superfluidity

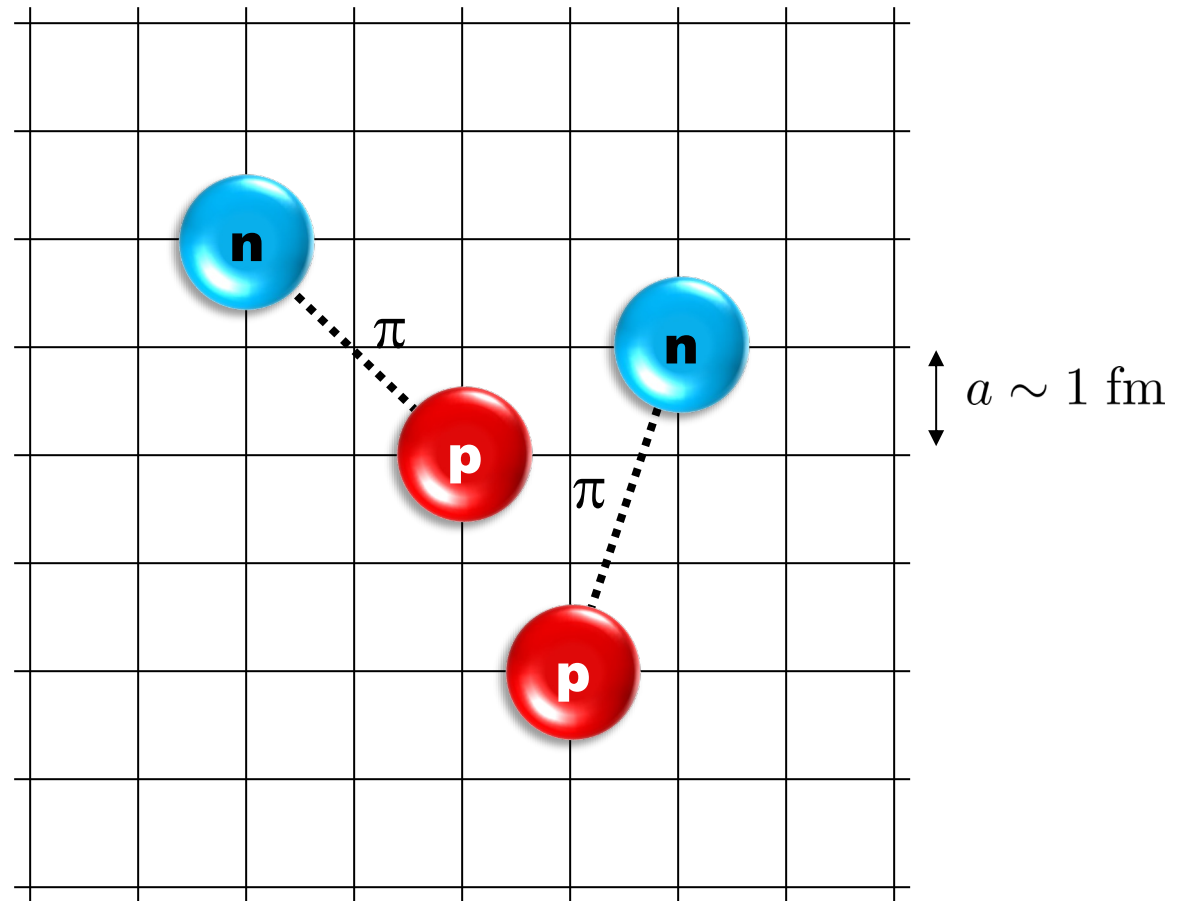
Neutron matter with N³LO interactions

Effective action

Experimental evidence

Summary and outlook

Lattice effective field theory

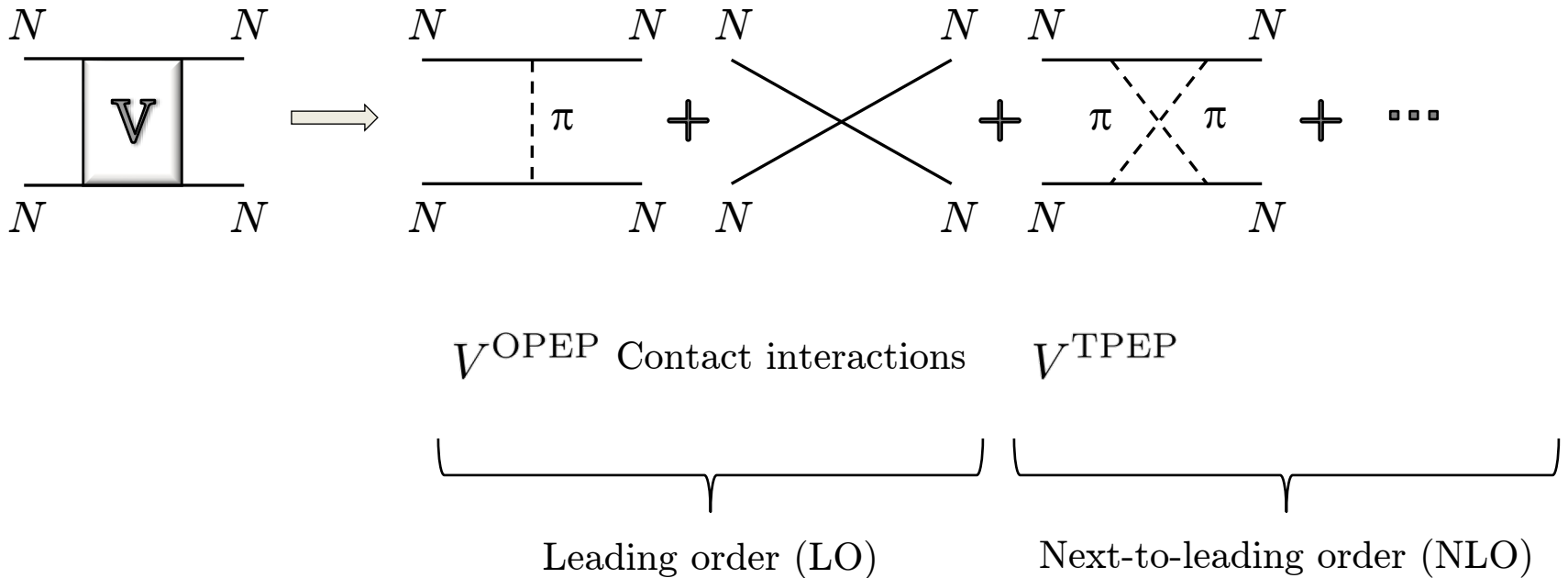


D.L, Annu. Rev. Nucl. Part. Sci. 75, 109 (2025)

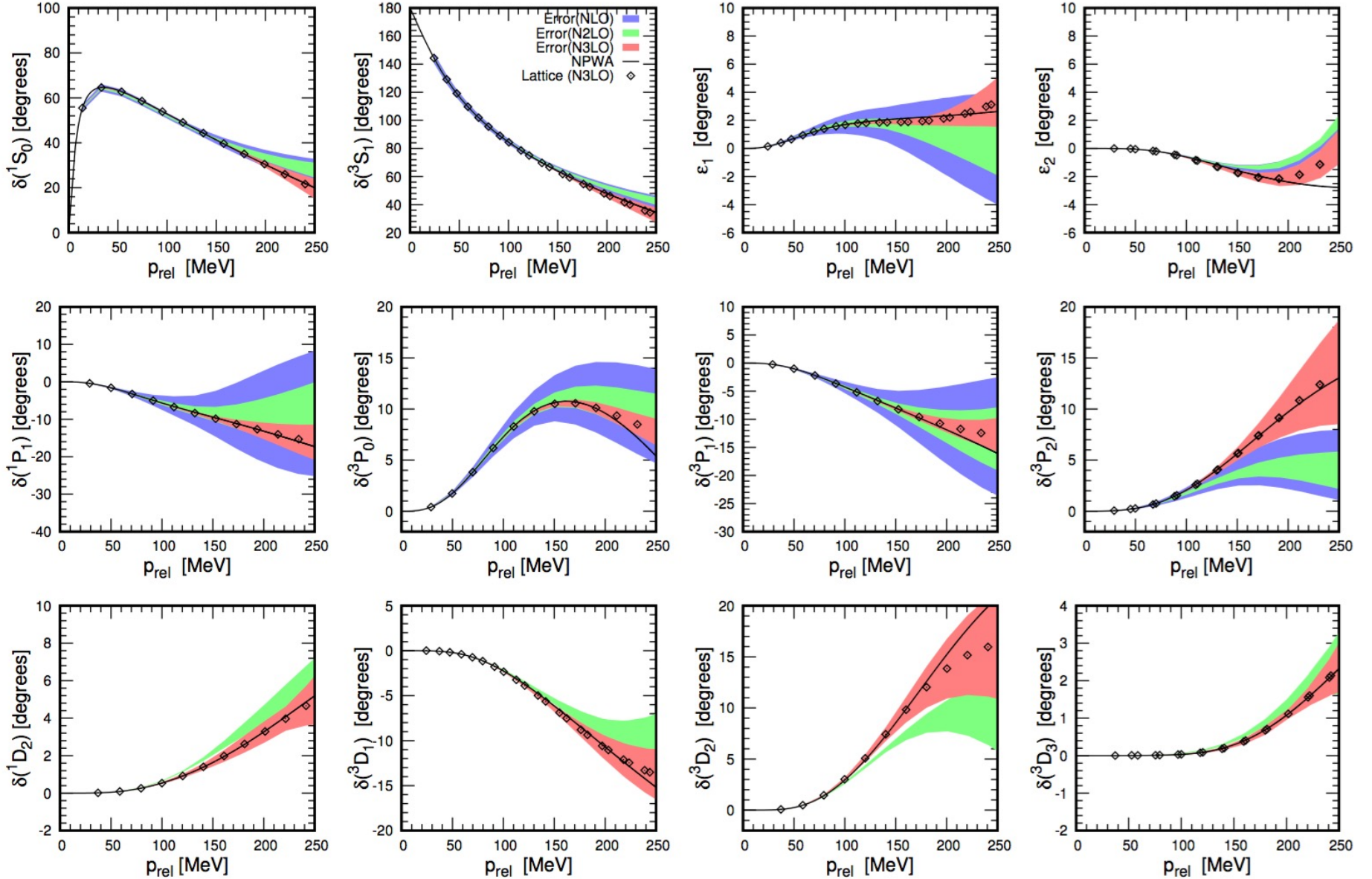
Lähde, Meißner, Nuclear Lattice Effective Field Theory (2019), Springer

Chiral effective field theory

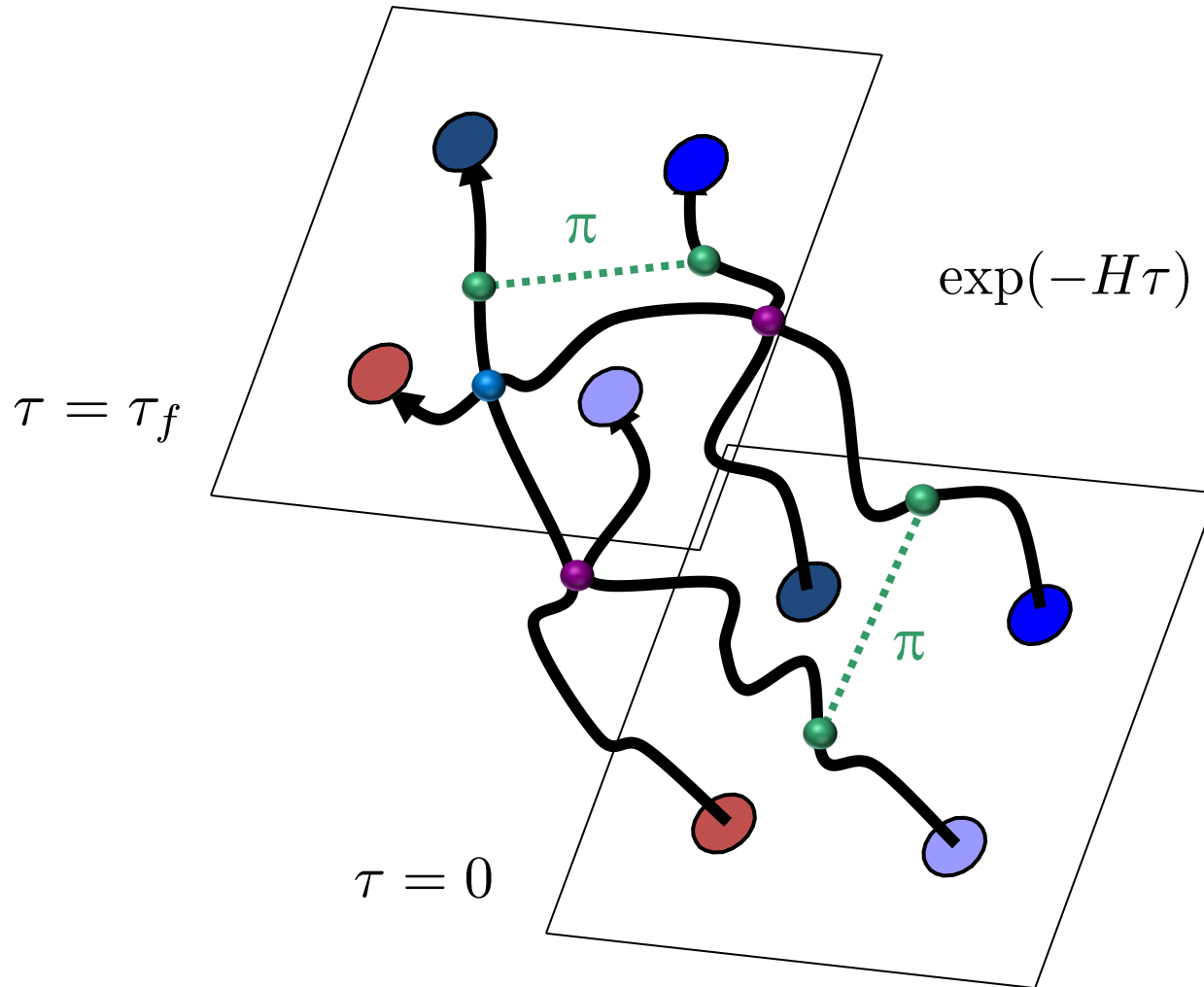
Construct the effective potential order by order



$a = 1.315$ fm



Euclidean time projection

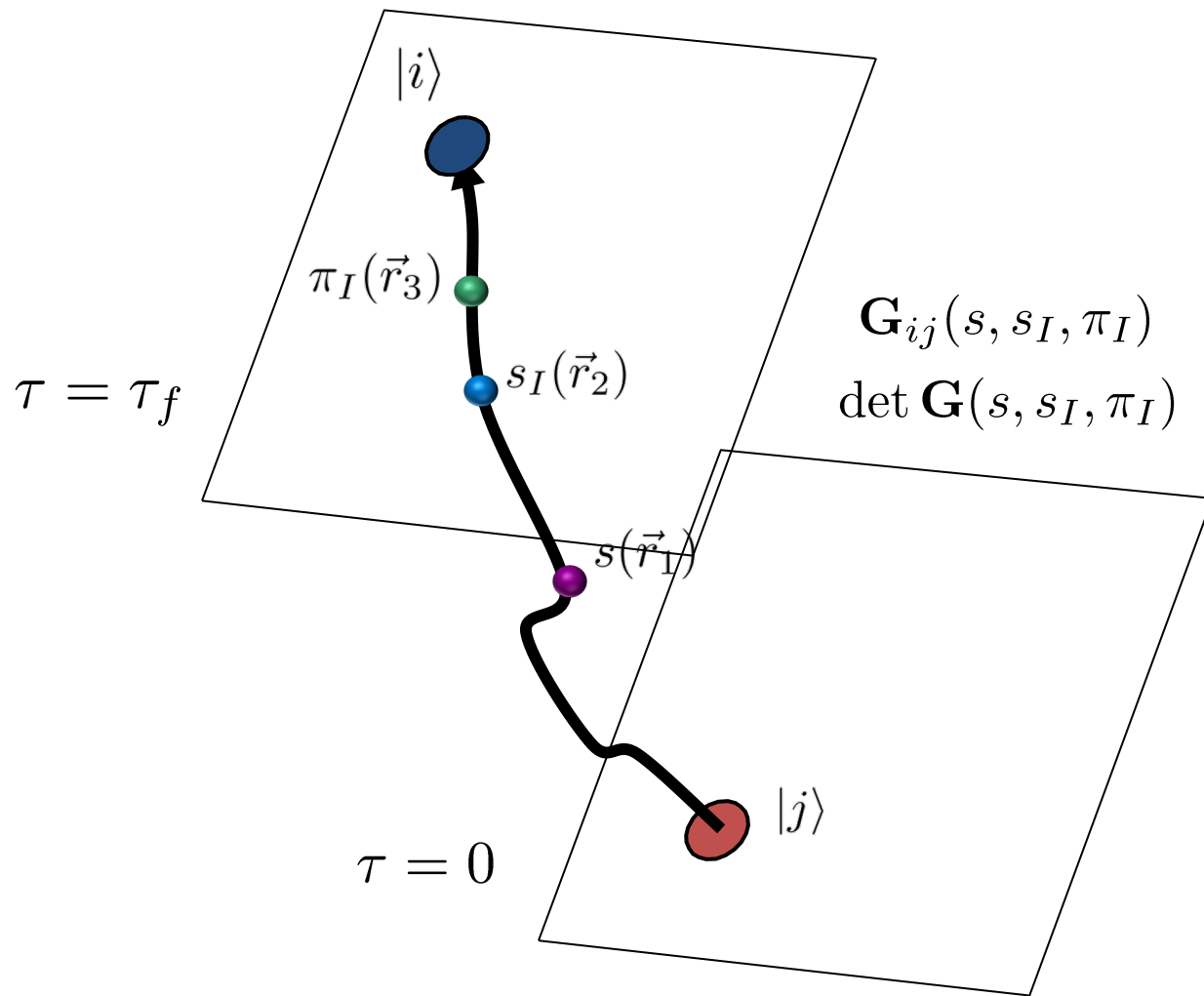


Auxiliary field method

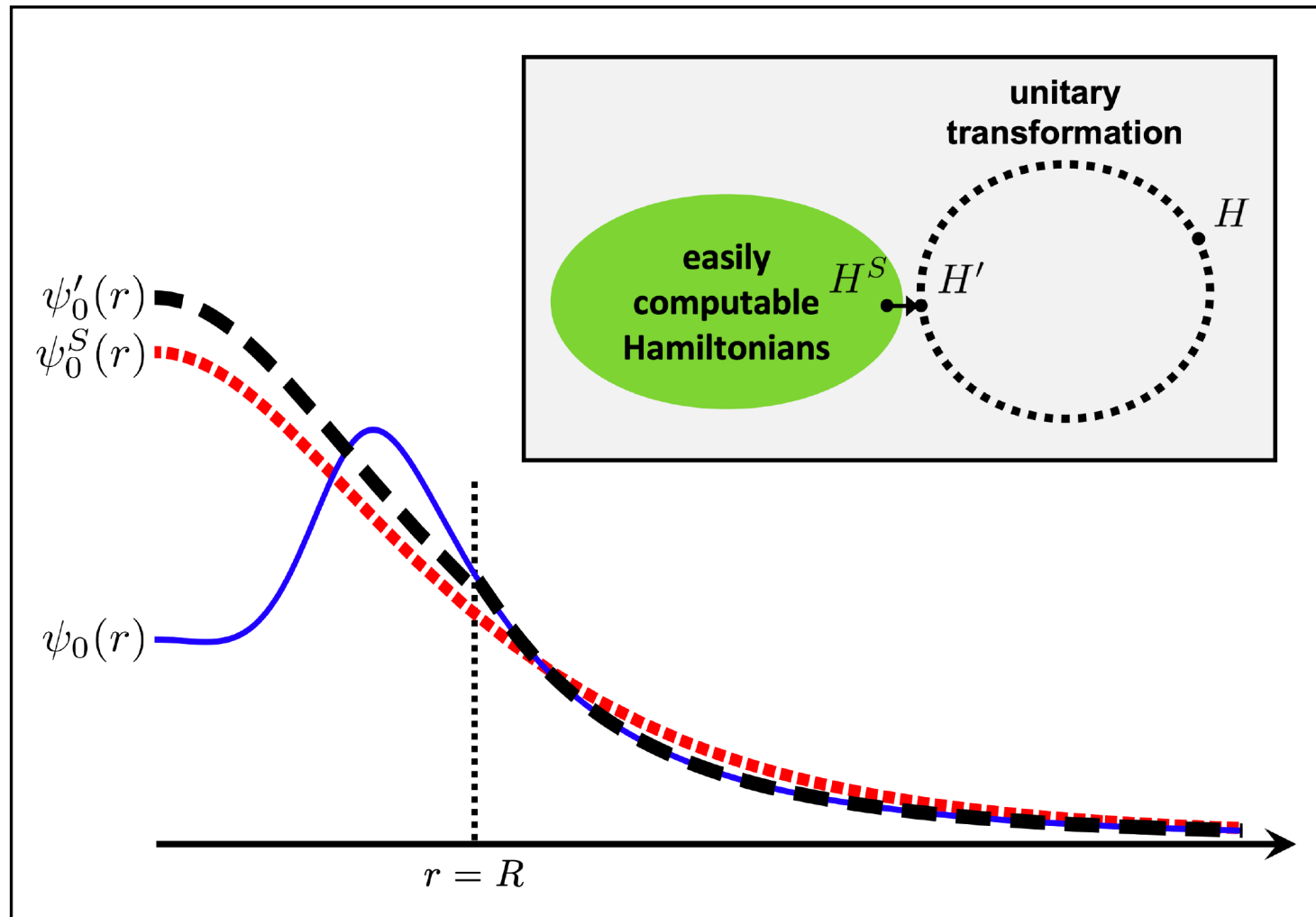
We can write exponentials of the interaction using a Gaussian integral identity

$$\begin{aligned} & \exp \left[-\frac{C}{2} (N^\dagger N)^2 \right] \quad \times \quad (N^\dagger N)^2 \\ &= \sqrt{\frac{1}{2\pi}} \int_{-\infty}^{\infty} ds \exp \left[-\frac{1}{2} s^2 + \sqrt{-C} s (N^\dagger N) \right] \quad \rangle \quad s N^\dagger N \end{aligned}$$

We remove the interaction between nucleons and replace it with the interactions of each nucleon with a background field.

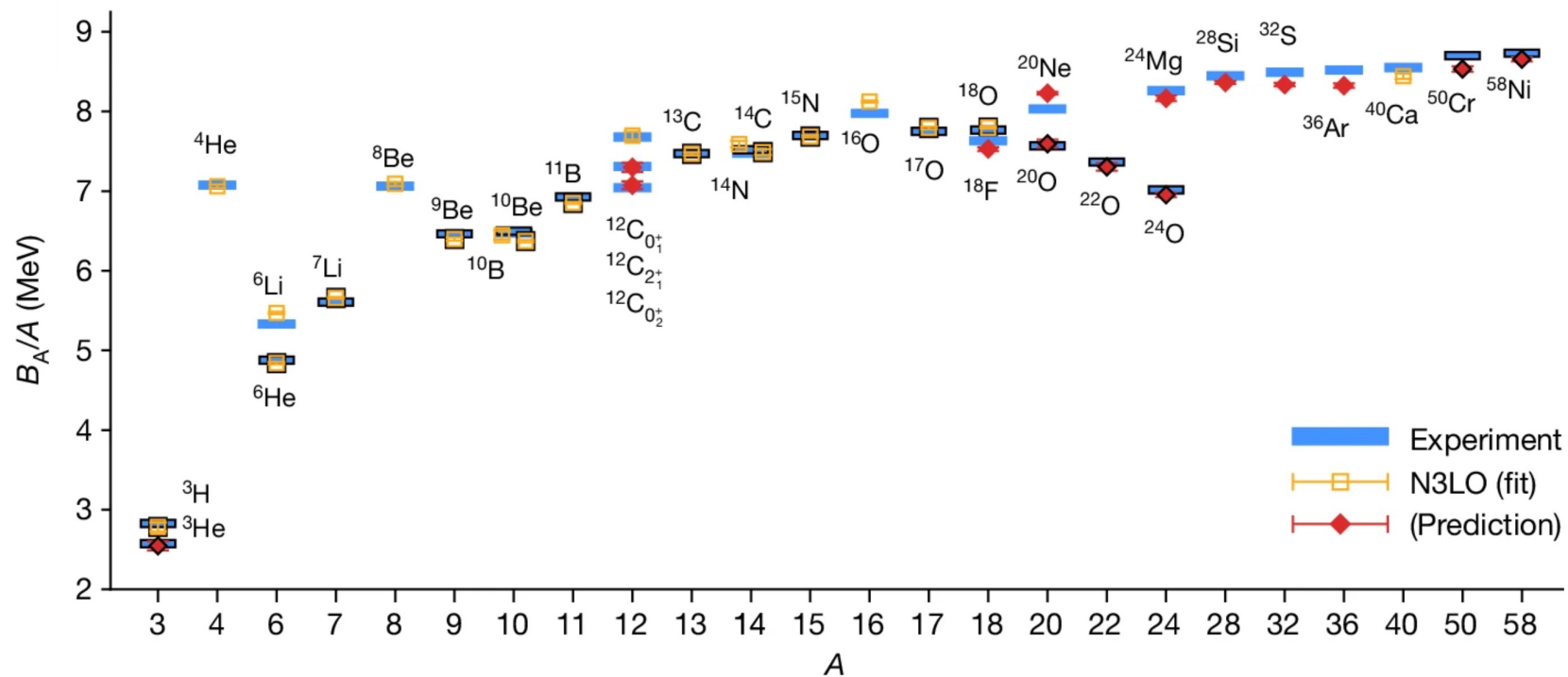


Wavefunction matching



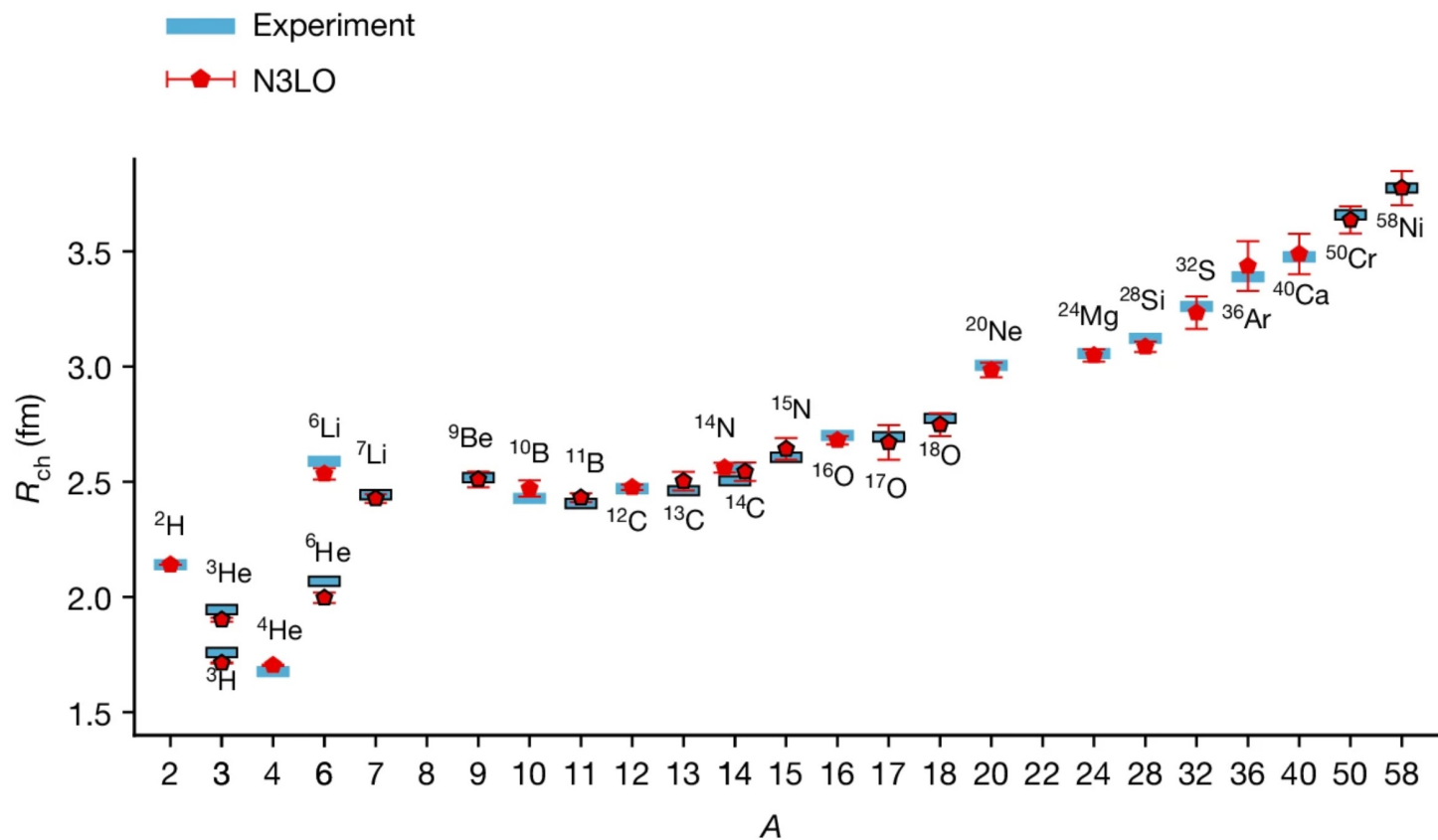
Elhatisari, Bovermann, Ma, Epelbaum, Frame, Hildenbrand, Krebs, Lähde, D.L., Li, Lu, M. Kim, Y. Kim, Meißner, Rupak, Shen, Song, Stellin, Nature 630, 59 (2024)

Binding energies



Elhatisari, Bovermann, Ma, Epelbaum, Frame, Hildenbrand, Krebs, Lähde, D.L., Li, Lu, M. Kim, Y. Kim, Meißner, Rupak, Shen, Song, Stellin, Nature 630, 59 (2024)

Charge radii



Elhatisari, Bovermann, Ma, Epelbaum, Frame, Hildenbrand, Krebs, Lähde, D.L., Li, Lu, M. Kim, Y. Kim, Meißner, Rupak, Shen, Song, Stellin, Nature 630, 59 (2024)

Neutron and nuclear matter

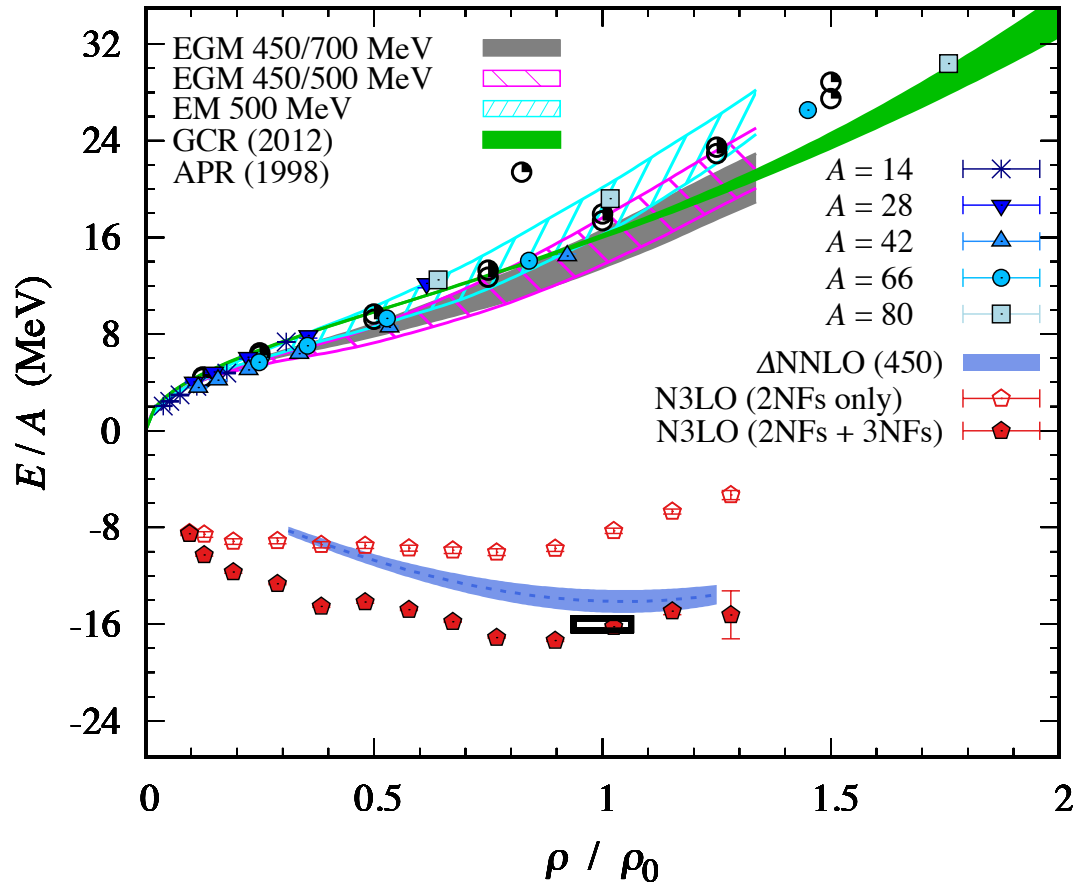
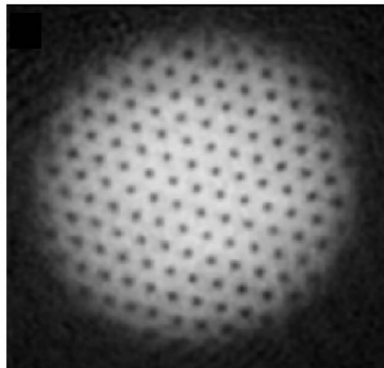


Figure adapted from Tews, Krüger, Hebeler, Schwenk, Phys. Rev. Lett. 110, 032504 (2013)

Elhatisari, Bovermann, Ma, Epelbaum, Frame, Hildenbrand, Krebs, Lähde, D.L., Li, Lu, M. Kim, Y. Kim, Meißner, Rupak, Shen, Song, Stellin, Nature 630, 59 (2024)

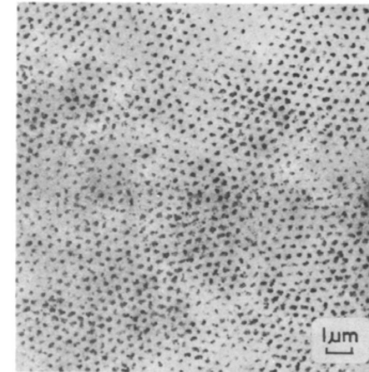
Superfluid condensation

BEC Theory



Ketterle, Zwierlein,
Ultracold Fermi Gases (2008)

BCS Theory



Essmann, Träuble,
Physics Letters A 27, 3 (1968)



Superfluid condensation

Bosonic superfluidity

$$\langle \Psi_0 | a^\dagger(\mathbf{r}) a(\mathbf{0}) | \Psi_0 \rangle$$

Fermionic superfluidity (S-wave)

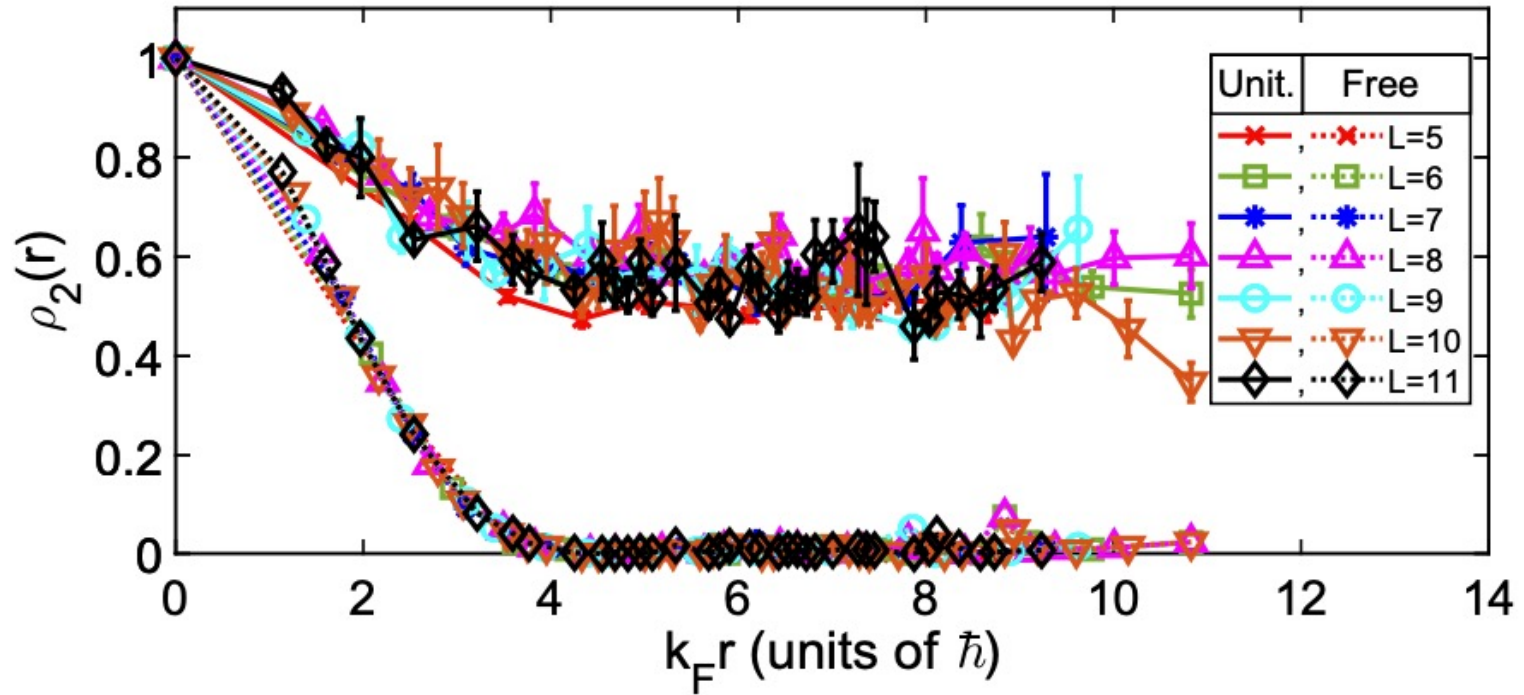
$$\langle \Psi_0 | a_\downarrow^\dagger(\mathbf{r}) a_\uparrow^\dagger(\mathbf{r}) a_\uparrow(\mathbf{0}) a_\downarrow(\mathbf{0}) | \Psi_0 \rangle$$

Fermionic superfluidity (P-wave)

$$\langle \Psi_0 | a_\uparrow^\dagger(\mathbf{r}) a_\uparrow^\dagger(\mathbf{r} + \Delta\mathbf{r}) a_\uparrow(\Delta\mathbf{r}) a_\uparrow(\mathbf{0}) | \Psi_0 \rangle$$

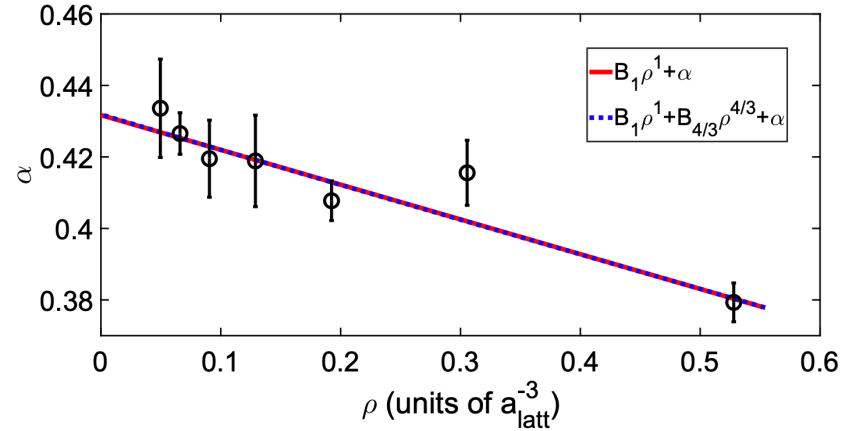
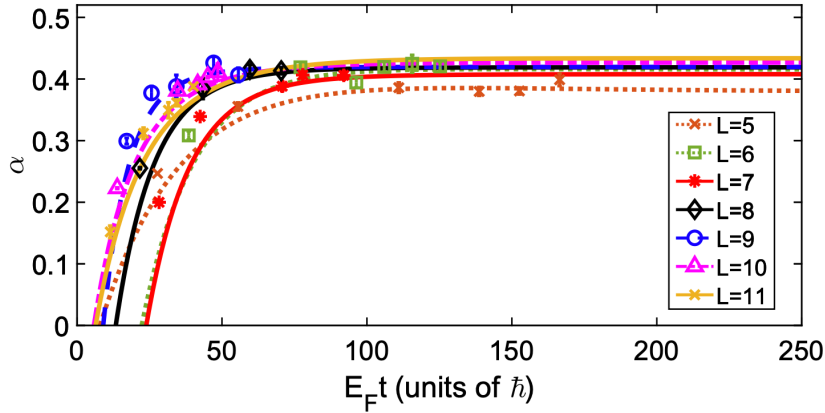
We can also perform calculations in momentum space. But we need to compute cumulants to obtain irreducible contributions only.

Unitary limit



He, Li, Lu, D.L., Phys. Rev. A 101, 063615 (2020)

Unitary limit



condensate fraction = 0.43(2)

He, Li, Lu, D.L., Phys. Rev. A 101, 063615 (2020)

${}^6\text{Li}$ experiments: 0.46(7) [1, 2] and 0.47(7) [3]

[1] Zwierlein, Stan, Schunck, Raupach, Kerman, Ketterle, PRL 92, 120403 (2004).

[2] Zwierlein, Schunck, Stan, Raupach, Ketterle, PRL 94, 180401 (2005).

[3] Kwon, Pace, Panza, Inguscio, Zwirger, Zaccanti, Scazza, Roati, Science 369, 84 (2020).

Can a many-body system have S-wave and P-wave superfluid condensation at the same time?

Generalized attractive extended Hubbard models

We consider generalized attractive extended (GAE) Hubbard models for two-component fermions in 1, 2, 3 dimensions

$$H = H_{\text{free}} + \frac{1}{2}C_2 \sum_{\mathbf{n}} \tilde{\rho}(\mathbf{n})^2$$

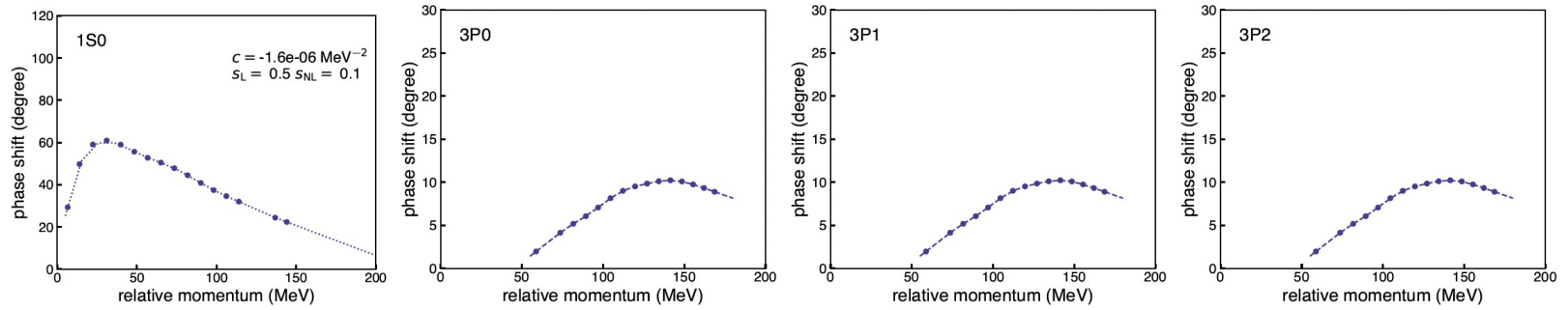
$$\tilde{\rho}(\mathbf{n}) = \sum_{j=\uparrow,\downarrow} \tilde{a}_j^\dagger(\mathbf{n})\tilde{a}_j(\mathbf{n}) + s_L \sum_{|\mathbf{n}-\mathbf{n}'|=1} \sum_{j=\uparrow,\downarrow} \tilde{a}_j^\dagger(\mathbf{n}')\tilde{a}_j(\mathbf{n}')$$

$$\tilde{a}_j(\mathbf{n}) = a_j(\mathbf{n}) + s_{NL} \sum_{|\mathbf{n}-\mathbf{n}'|=1} a_j(\mathbf{n}')$$

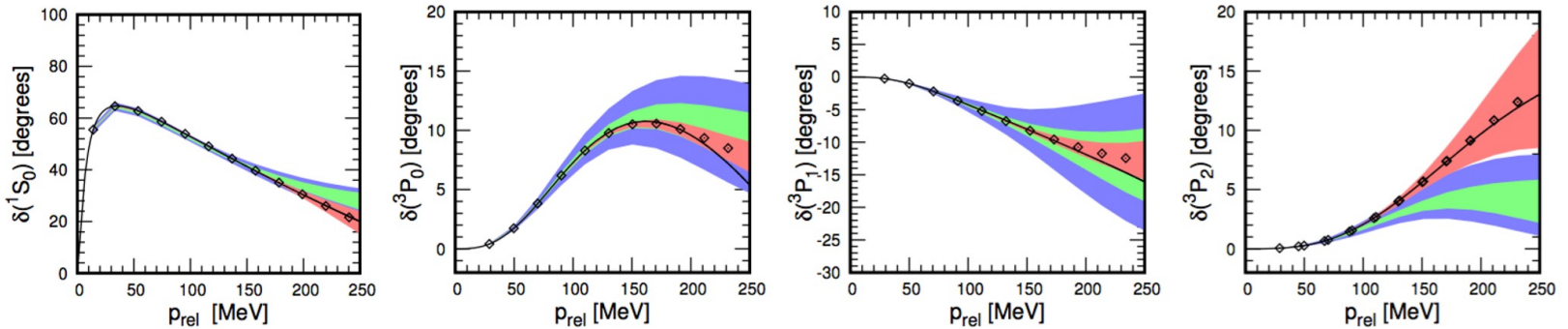
This interaction produces both S-wave and P-wave attraction. The symmetry group is

$$G = \text{U}(1) \times \text{SU}(2)_{\text{spin}} \times \text{SO}(3)_{\text{orb}}$$

3D GAE Hubbard model



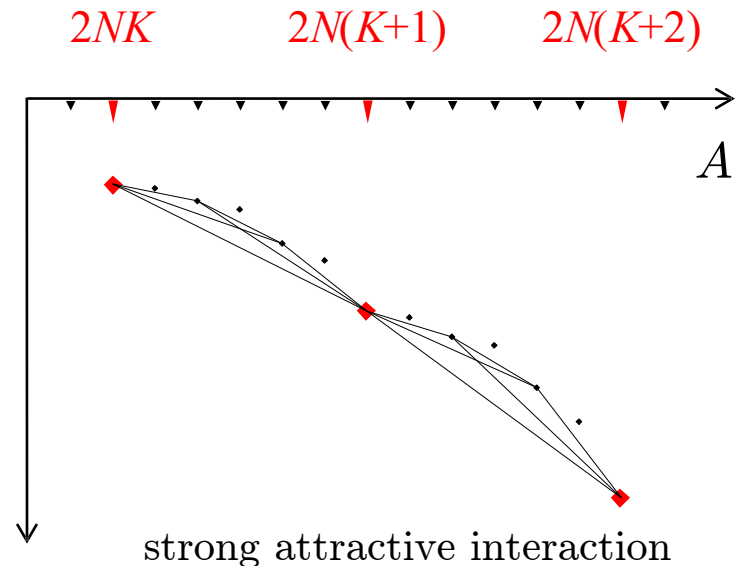
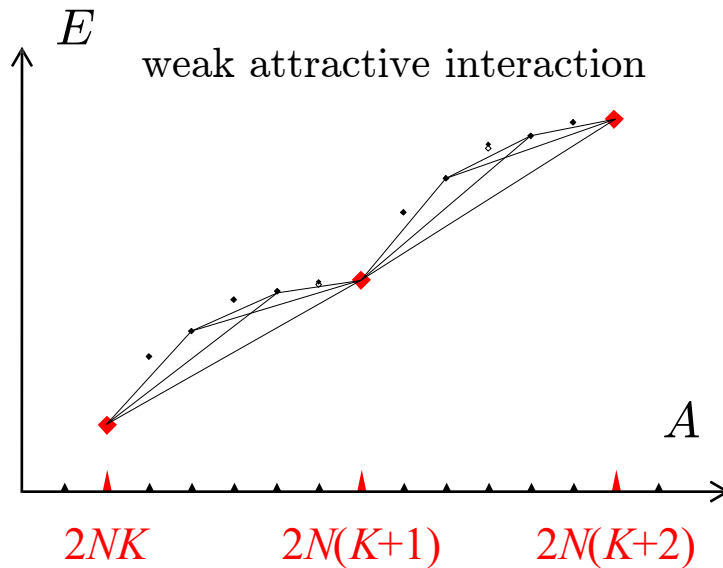
Comparison with N3LO chiral



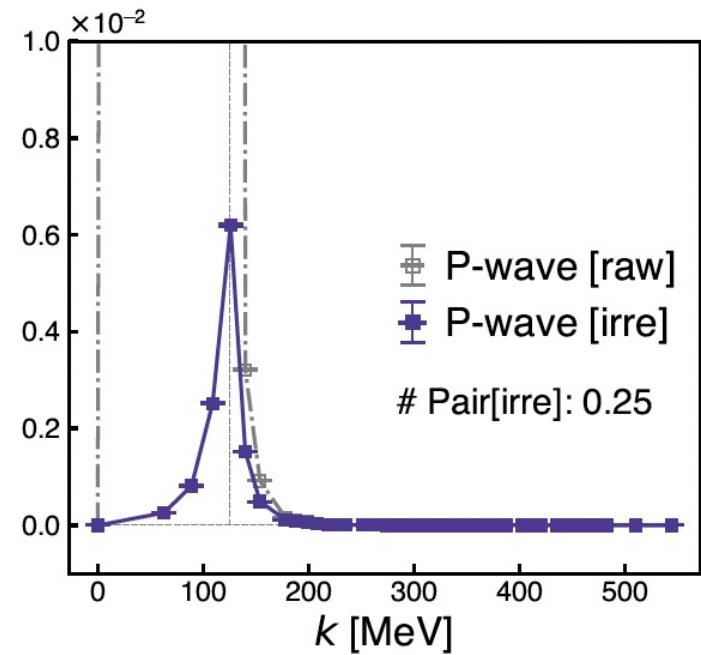
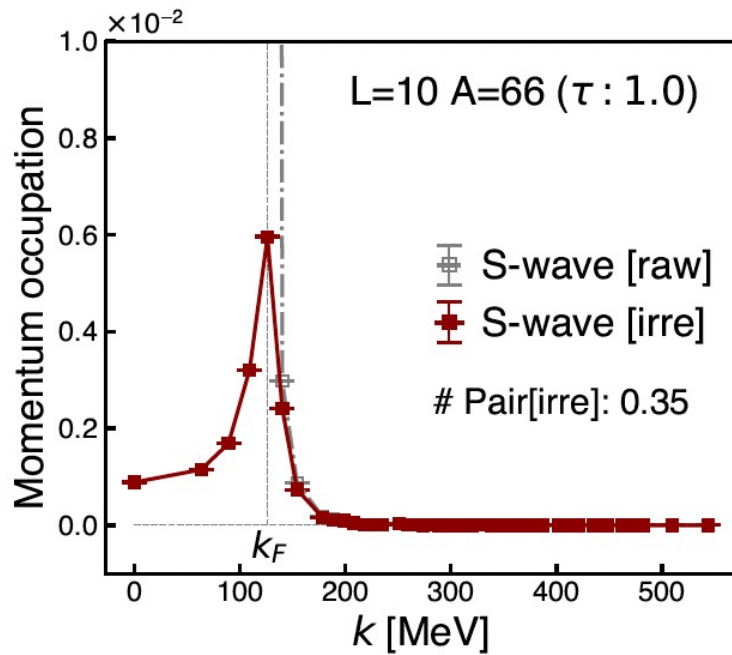
Spectral convexity theorem

Consider any fermionic system with an $SU(2N)$ symmetry with purely attractive interactions. It must obey the $SU(2N)$ convexity bounds illustrated below, and the $SU(2N)$ symmetry is not spontaneously broken.

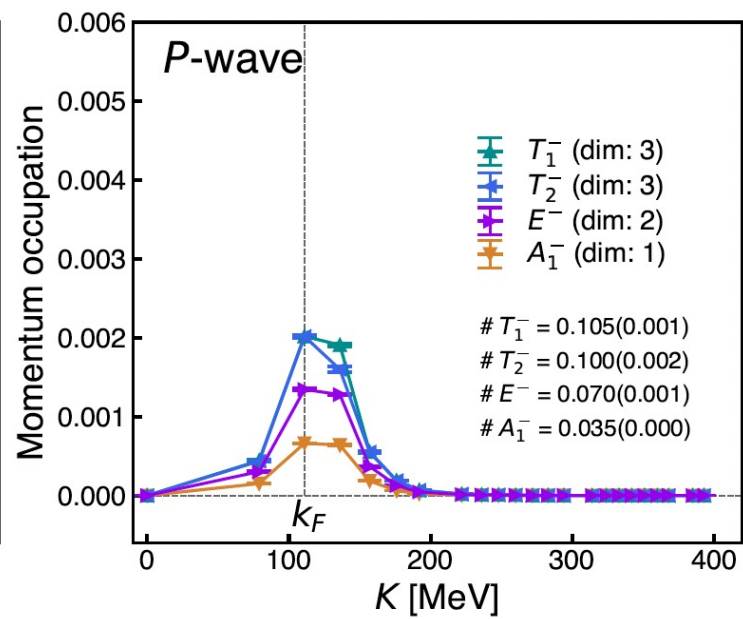
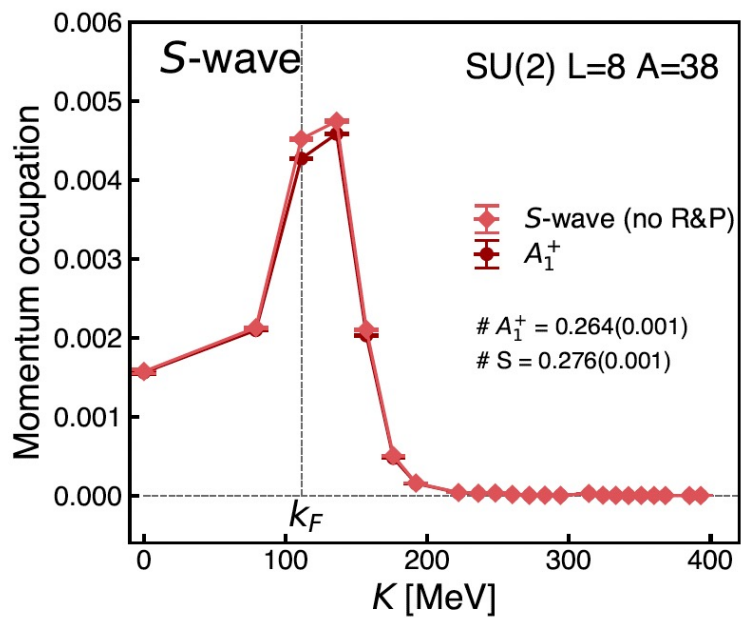
D.L., Phys. Rev. Lett. 98 (2007) 182501

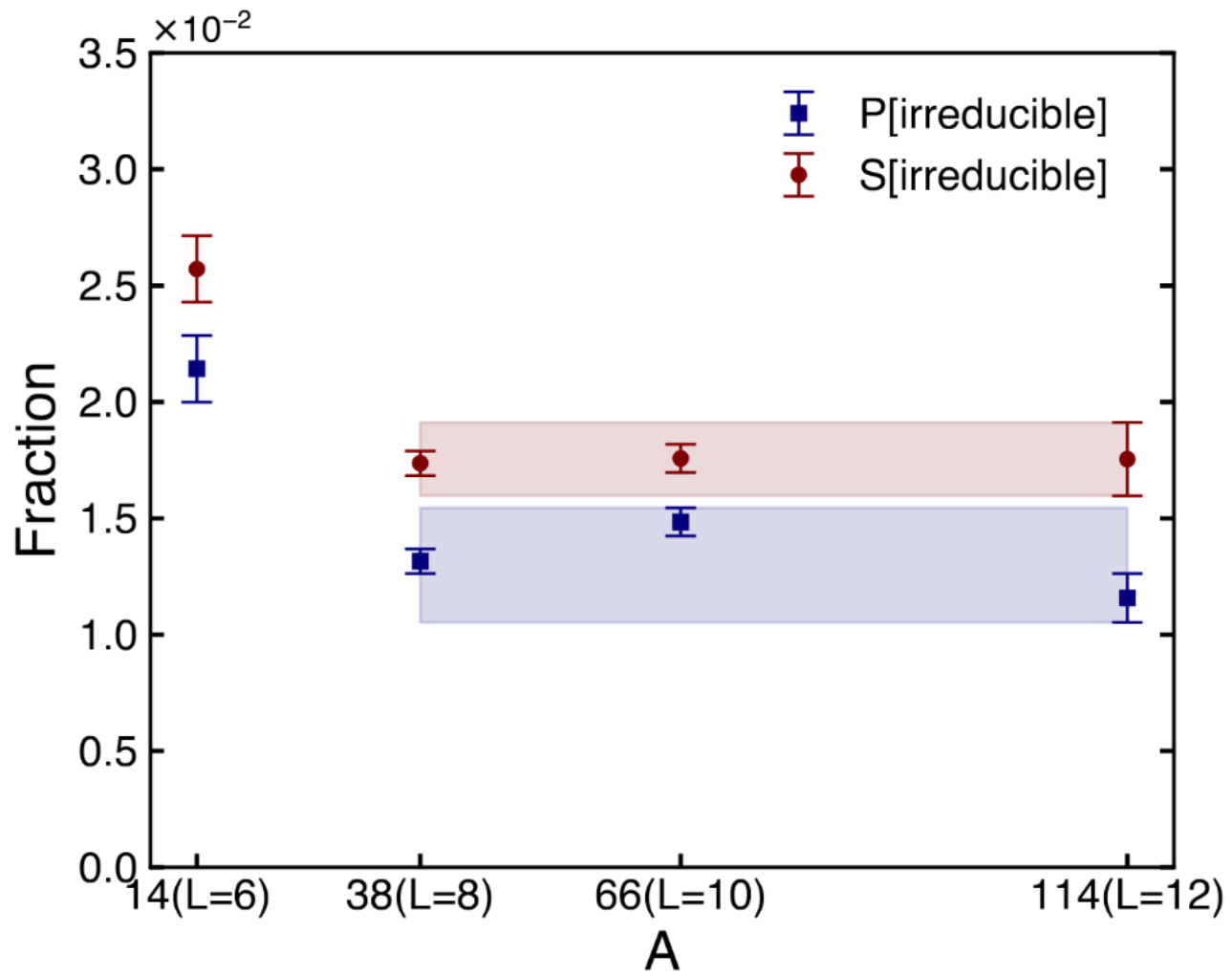


GAE Hubbard model



arXiv:2602.17611

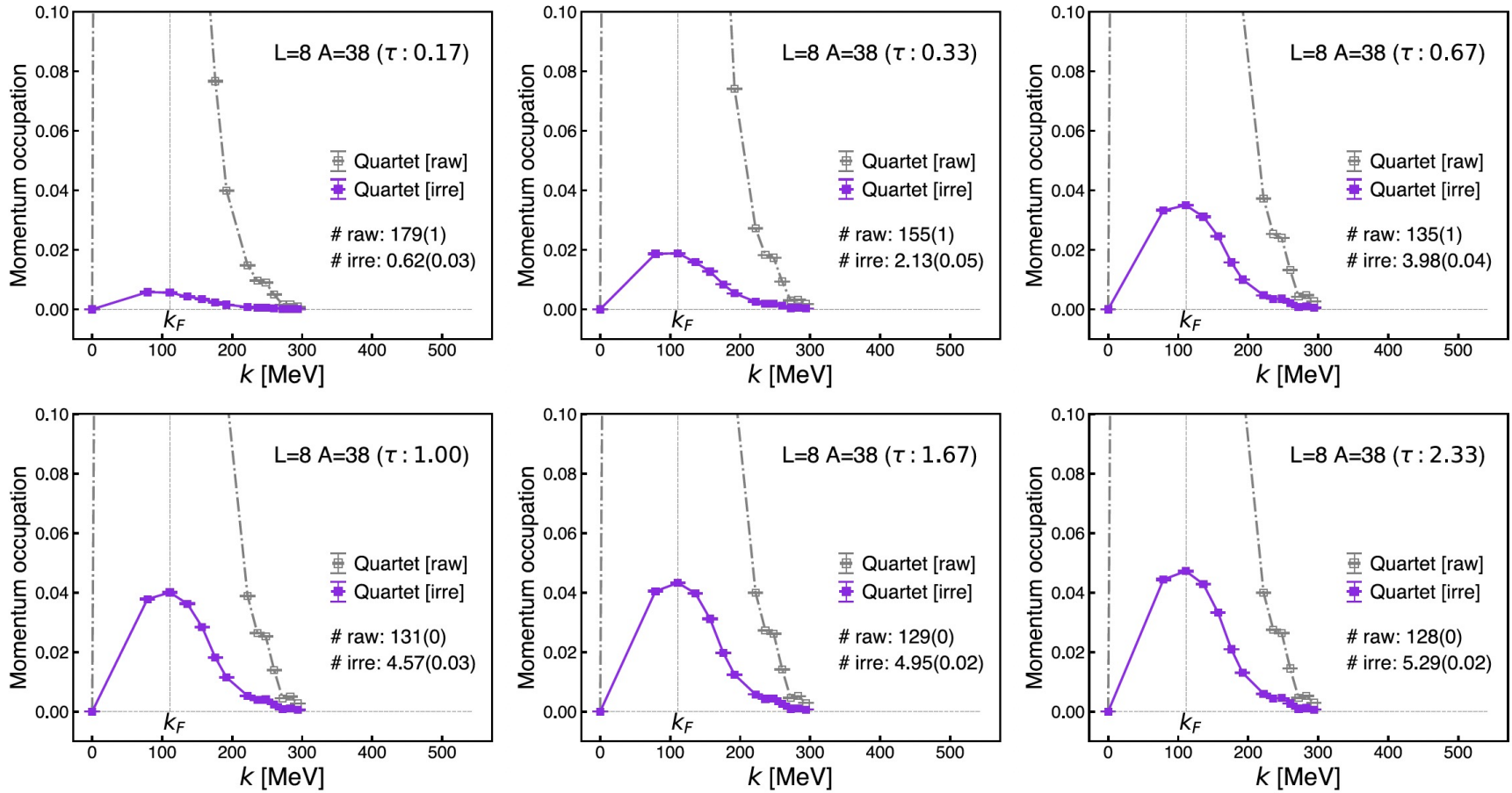




How does the $SU(2)$ spin symmetry remain unbroken if there is a P-wave condensate?

Why are the S-wave and P-wave condensates so small?

GAE Hubbard model



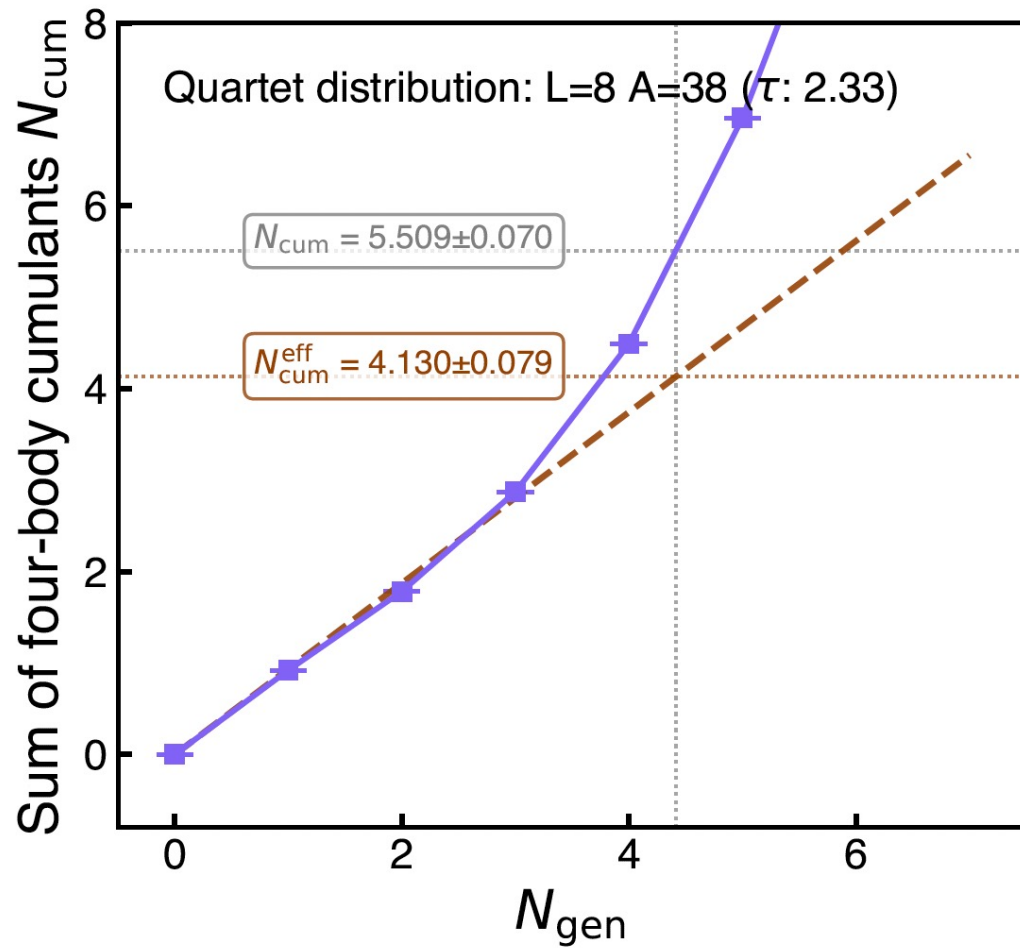


Table 1. Condensate fractions for the 3D GAE Hubbard model. *Ab initio* lattice results for the condensate fractions for s-wave pairs, p-wave pairs, and quartets for $c = -1.6 \times 10^{-6} \text{ MeV}^{-2}$, $s_L = 0.5$ and $s_{NL} = 0.1$.

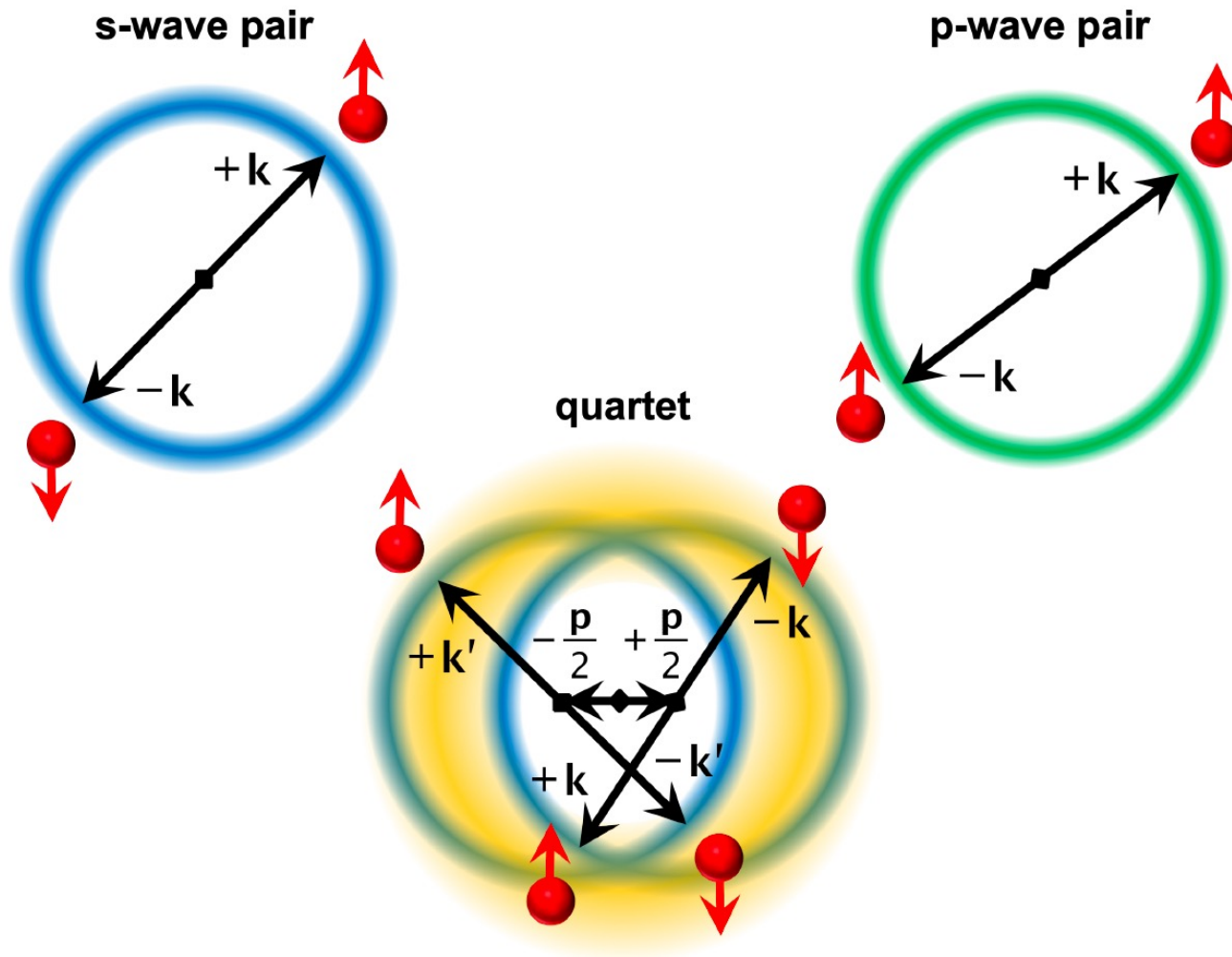
L	A	density (fm^{-3})	$2 \times \text{S-wave}/A$	$2 \times \text{P-wave}/A$	$4 \times \text{Quartets}/A$
6	14	0.0084	0.0253 (1)	0.0217 (1)	0.0034 (3)
8	38	0.0097	0.0169 (3)	0.0130 (2)	0.4347 (83)
10	66	0.0086	0.0177 (5)	0.0147 (7)	0.4759 (207)
12	114	0.0086	0.0217 (34)	0.0105 (13)	not calculated

S-wave pairs 1.8(4)%
P-wave pairs 1.3(3)%
quartets 45(3)%

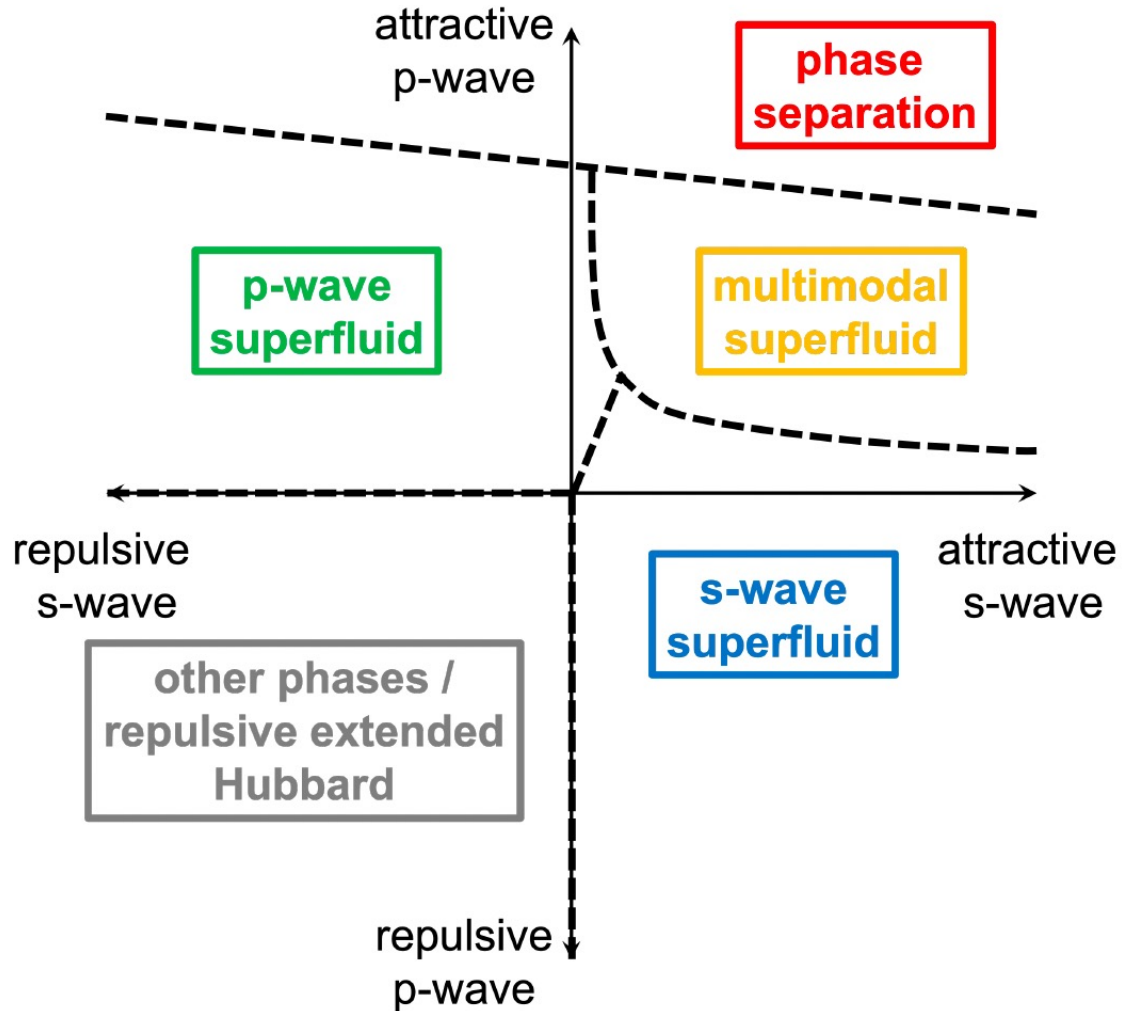
Table S9. SU(2) lattice energies for $L^3 = 10^3$. Lattice SU(2) energies calculated with $c = -1.6 \times 10^{-6} \text{ MeV}^{-2}$, $s_L = 0.5$, and $s_{\text{NL}} = 0.1$. For $A = 66$, the density is $\rho = 8.5898 \times 10^{-3} \text{ fm}^{-3}$, corresponding to a Fermi momentum $k_F = 125.66 \text{ MeV}$.

A	E_{SU2} (MeV)	2Δ (MeV)	$4\Delta_Q$ (MeV)
66	84.88 (11)		
67	88.27 (13)		
68 $\uparrow\downarrow$	89.07 (19)	2.59 (34)	
68 $\uparrow\uparrow$	90.65 (21)	1.01 (35)	
70	92.10 (28)		1.17 (48)

Multimodal superfluidity

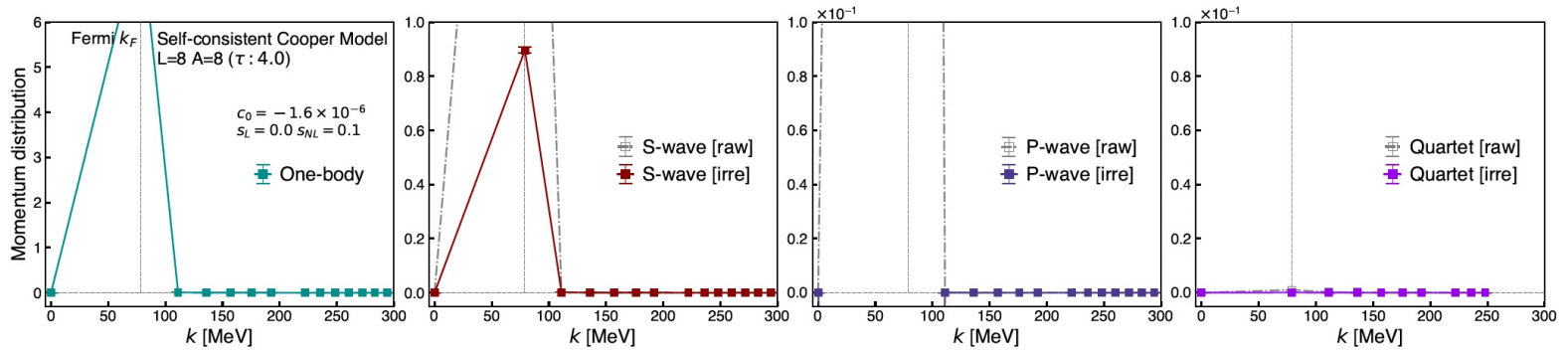


Quantum phase diagram

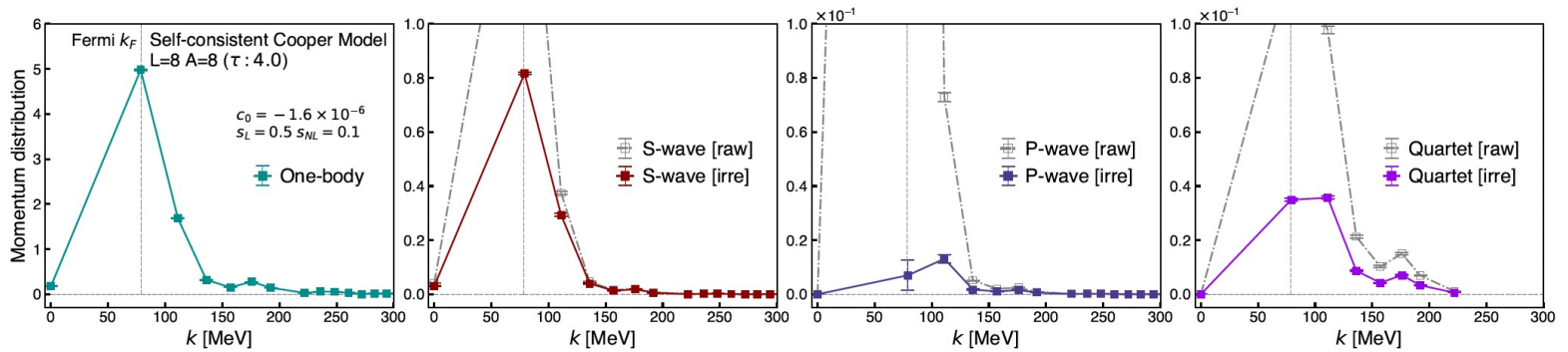


Self-consistent Cooper model

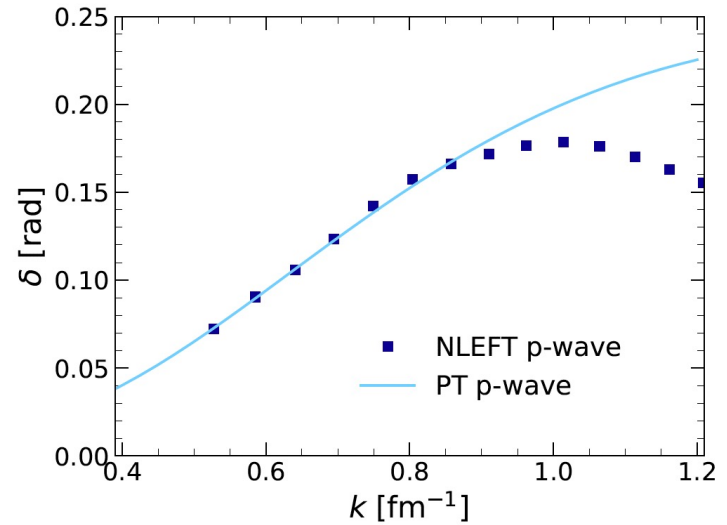
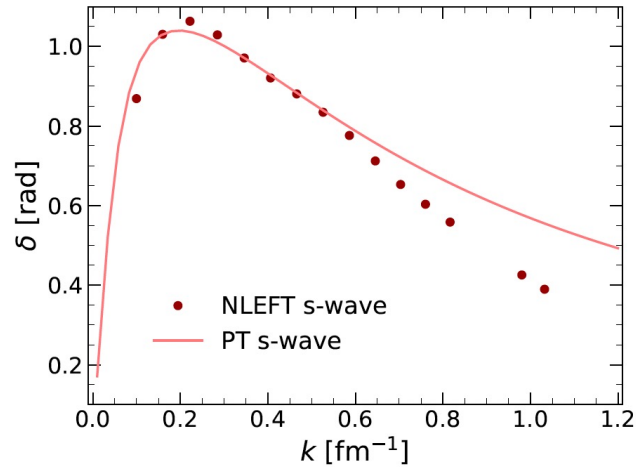
S-wave interactions only



S-wave and P-wave interactions



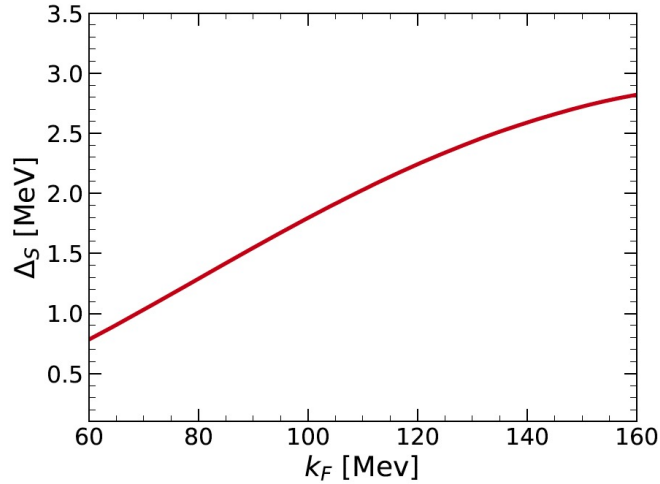
BCS gap equation



$$V(r) = \frac{\hbar^2}{m} \frac{\beta^2 \lambda(\lambda-1)}{\cosh^2(\beta r)}$$

Spin-balanced system

Continuum BCS gap



Self-consistent lattice Cooper model

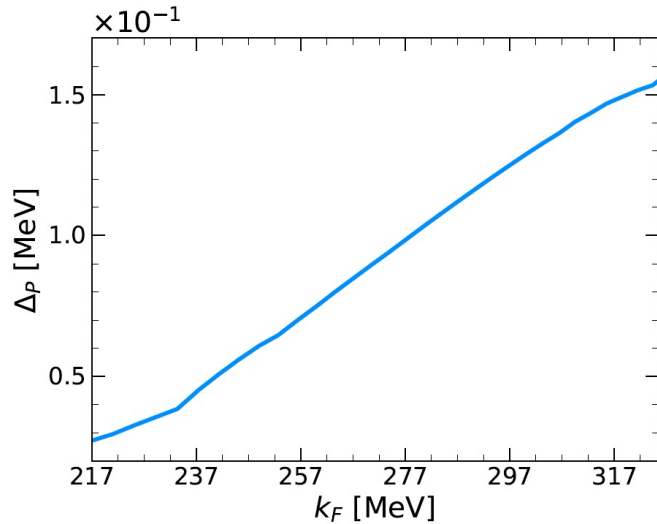
Lattice size	L=4	L=5	L=6	L=7	L=8
k_F (MeV)	157.08	125.66	104.72	89.76	78.54
Δ (MeV)	2.1372	1.8763	1.6147	1.3760	1.1713
$(E_{\text{free}} - E_{\uparrow\downarrow}^{\text{latt}})/2$	2.10 (1)	1.87 (4)	1.61 (3)	1.36 (1)	1.19 (4)
$(E_{\text{free}} - E_{\uparrow\uparrow}^{\text{latt}})/2$	0.56 (2)	0.39 (6)	0.32 (6)	0.27 (18)	0.02 (25)
$(2E_2 - E_4^{\text{latt}})/4$	1.23 (1)	0.63 (1)	0.32 (1)	0.17 (2)	0.10 (1)

Many-body lattice

A	E_{SU2} (MeV)	2Δ (MeV)	$4\Delta_Q$ (MeV)
66	84.88 (11)		
67	88.27 (13)		
68 $\uparrow\downarrow$	89.07 (19)	2.59 (34)	
68 $\uparrow\uparrow$	90.65 (21)	1.01 (35)	
70	92.10 (28)		1.17 (48)

Spin-polarized system

Continuum BCS gap



Self-consistent lattice Cooper model

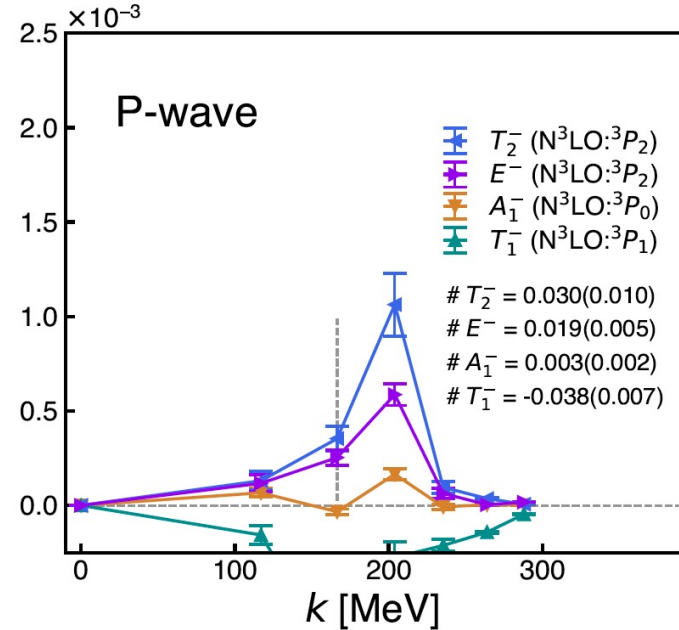
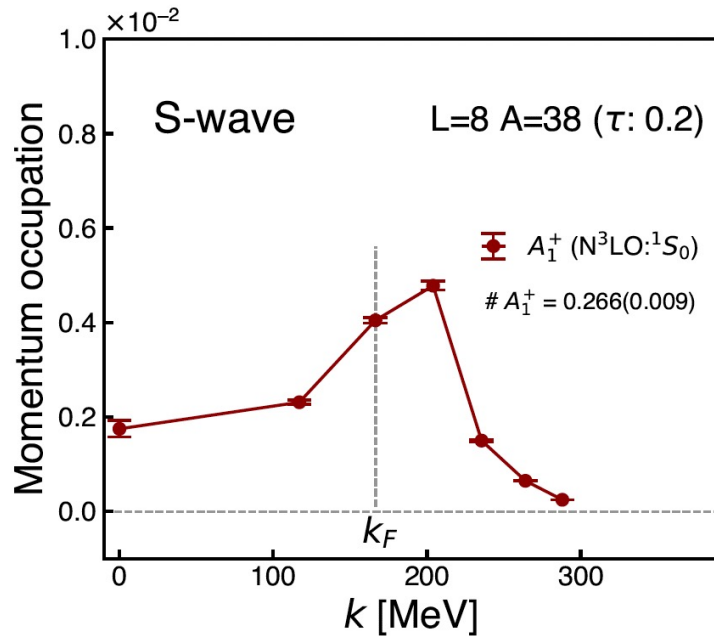
Lattice size	$L = 6$	$L = 8$	$L = 10$	$L = 15$	$L = 16$	$L = 17$
k_F (MeV)	104.72	111.07	125.66	225.57	222.14	221.76
Δ_P^{ax} (MeV)	0.2077	0.2094	0.0550	0.0358	0.0412	0.0471

Many-body lattice

(L, A)	$E_{\text{SU}(2)}$ (MeV)	$2\Delta_P$ (MeV)
(8, 19)	75.42 (2)	
(8, 20)	82.55(2)	
(8, 21)	89.45 (2)	0.23 (4)
(10, 33)	126.62 (2)	
(10, 34)	133.97 (2)	
(10, 35)	141.19 (2)	0.13 (5)

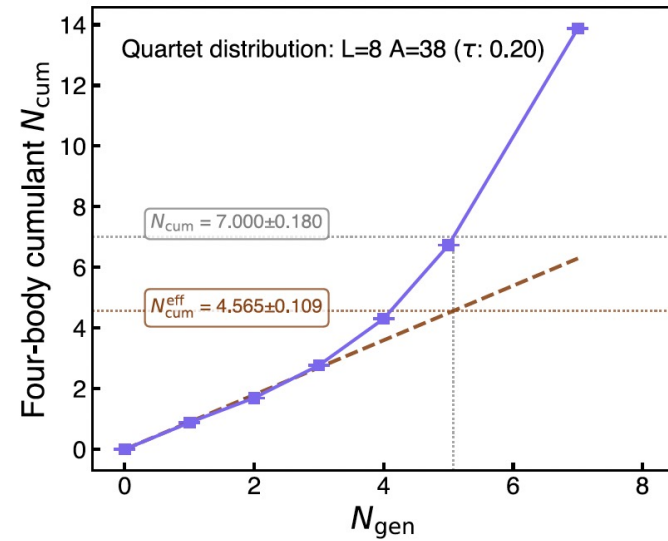
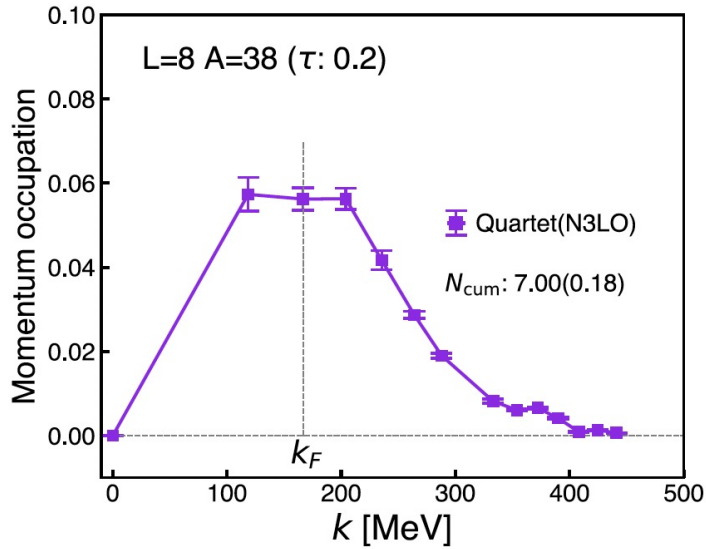
Neutron matter with N3LO interactions

$$k_F = 167 \text{ MeV}$$



Neutron matter with N3LO interactions

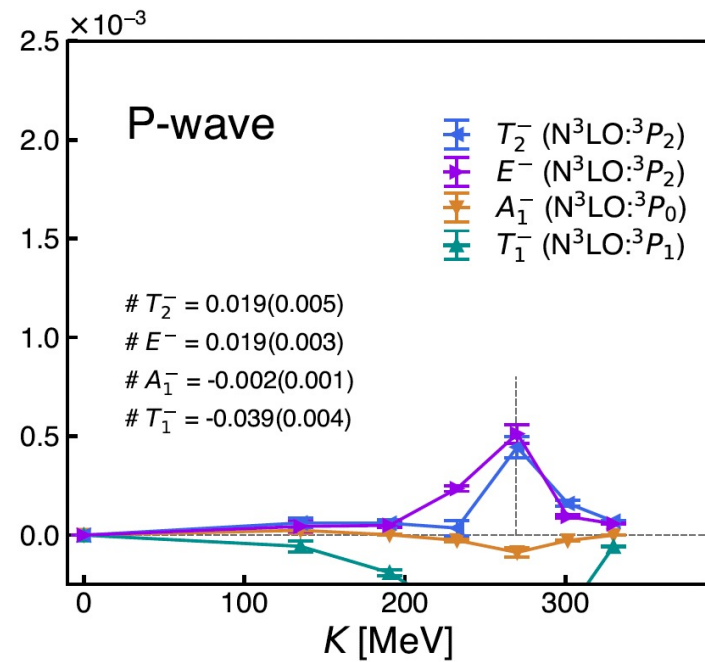
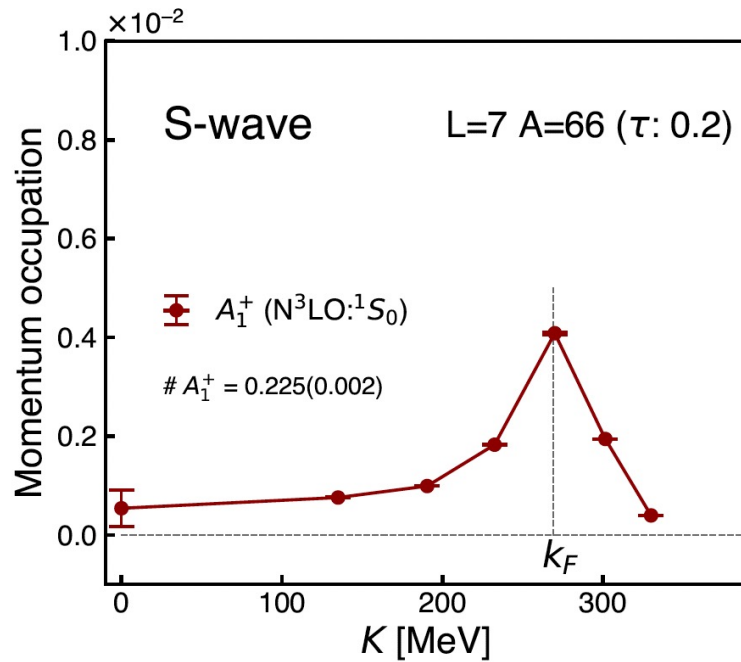
$$k_F = 167 \text{ MeV}$$



s-wave pairs 1.40(5)%
 p-wave pairs ${}^3P_0 = 0.02(1)\%$, ${}^3P_2 = 0.26(8)\%$
 quartets 48(1)%

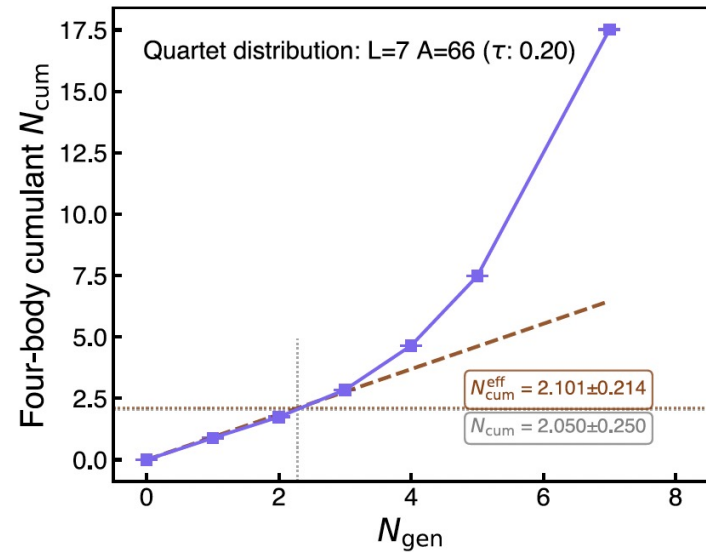
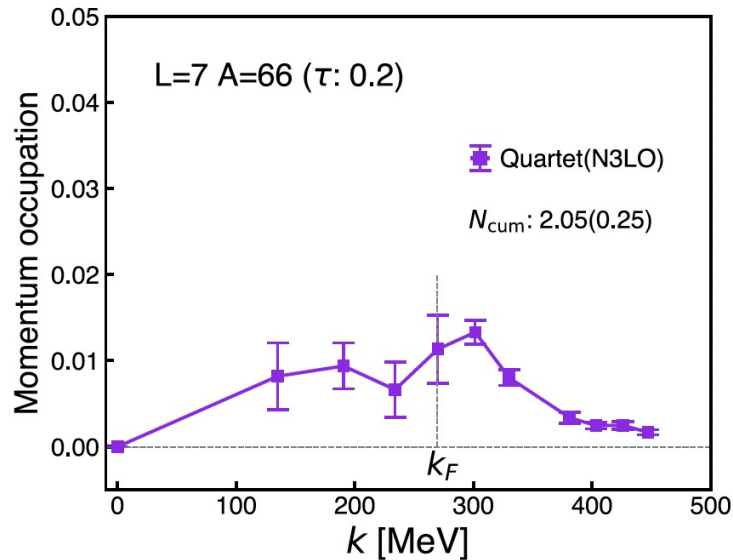
Neutron matter with N3LO interactions

$$k_F = 269 \text{ MeV}$$



Neutron matter with N3LO interactions

$$k_F = 269 \text{ MeV}$$



s-wave pairs 0.68(1)%
 p-wave pairs ${}^3P_0 = 0.00\%$, ${}^3P_2 = 0.12(2)\%$
 quartets 13(1)%

Effective action

We can write the interactions using auxiliary fields for the s-wave and p-wave pairing channels:

$$\phi, A_{\mu,j} \quad \begin{array}{l} \mu = 1, 2, 3 \text{ (orbital)} \\ j = 1, 2, 3 \text{ (intrinsic spin)} \end{array}$$

We integrate out the fermions and consider the terms in the low-energy effective action.

When the p-wave interaction is strong enough to bind two S-wave pairs, then we have asymptotic states composed of quartets. Our low-energy effective action must include an interpolating field for the quartet degrees of freedom.

$$Q_s \equiv \phi^2$$

$$D_1 \equiv \text{Tr}(AA^T) = \sum_{\mu,j} A_{\mu j} A_{\mu j},$$

$$D_2 \equiv \text{Tr}(A^\dagger A) = \sum_{\mu,j} A_{\mu j}^* A_{\mu j},$$

$$T_{jk}^{(3)} \equiv \sum_{\mu} A_{\mu j}^* A_{\mu k} - \frac{1}{3} \delta_{jk} D_2, \quad (\text{Spin Density Tensor})$$

$$T_{\mu\nu}^{(4)} \equiv \sum_j A_{\mu j} A_{\nu j} - \frac{1}{3} \delta_{\mu\nu} D_1, \quad (\text{Orbital Pair Tensor})$$

$$T_{jk}^{(5)} \equiv \sum_{\mu} A_{\mu j} A_{\mu k} - \frac{1}{3} \delta_{jk} D_1. \quad (\text{Spin Pair Tensor})$$

$$\begin{aligned} V_{\text{eff}} = & \mu_s |\phi|^2 + \frac{g_H}{2} |\phi|^4 + \alpha_s |Q_s|^2 + r_p D_2 + \sum_{i=1}^2 \beta_i |D_i|^2 \\ & + \beta_3 \text{Tr}[(T^{(3)})^2] + \beta_4 \text{Tr}[(T^{(4)})^\dagger T^{(4)}] + \beta_5 \text{Tr}[(T^{(5)})^\dagger T^{(5)}] \\ & - \frac{\eta_s}{2} [(\phi^\dagger)^2 Q_s + \text{h.c.}] + u_{sp} |\phi|^2 D_2 \\ & - \frac{\lambda_{sp}}{2} [Q_s^\dagger D_1 + \text{h.c.}] - \frac{\eta_{sp}}{2} [(\phi^\dagger)^2 D_1 + \text{h.c.}]. \end{aligned}$$

The S-wave pair field gets a nonzero expectation value.

$$\langle \phi \rangle = v = |v|e^{i\theta}$$

The couplings in the effective action produce a nonzero expectation value for the quartet field and double P-wave pair composite operator

$$\Sigma_s \equiv \langle Q_s \rangle = \left(\frac{\beta_1 \eta_s + \frac{1}{2} \lambda_{sp} \eta_{sp}}{2(\alpha_s \beta_1 - \frac{1}{4} \lambda_{sp}^2)} \right) v^2$$

$$\Sigma_1 \equiv \langle D_1 \rangle = \left(\frac{\alpha_s \eta_{sp} + \frac{1}{2} \lambda_{sp} \eta_s}{2(\alpha_s \beta_1 - \frac{1}{4} \lambda_{sp}^2)} \right) v^2$$

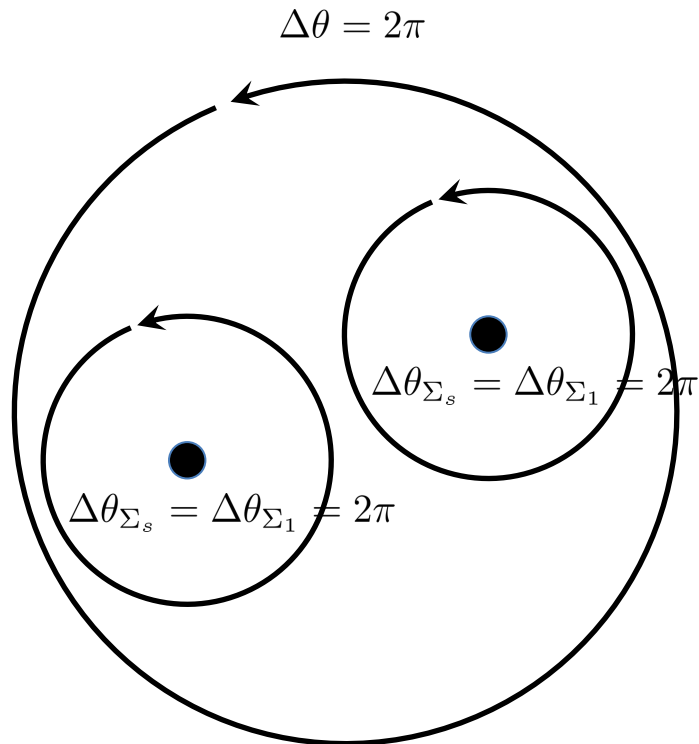
But the p-wave pair operator by itself has zero expectation value and the SU(2) spin symmetry and rotational symmetry are unbroken

$$\langle A_{\mu,j} \rangle = 0$$

We note that condensate phases are locked together:

$$\theta_{\Sigma_s} = \theta_{\Sigma_1} = 2\theta$$

We therefore have a rich phenomenology of vortices and half vortices with many metastable configurations that could appear in the crusts of neutron stars.



The phase locking of the s-wave pair condensate, p-wave double pair condensate, and quartet condensate results in a greater total superfluid stiffness. Because the coupled condensates must wind together, more energy is required to impose a macroscopic phase twist, which corresponds directly to an increase in the superfluid density.

There are low-energy spin excitations associated with the 3P_2 double pairs decoupling from each other. This allows for low-energy neutrino emission in older neutron stars.

There appear to be many interesting consequences of multimodal superfluidity for neutron star crust cooling and glitch dynamics.

Experimental evidence

S-wave pair binding in MeV

Nuclei	Predominant Orbitals	$2\Delta_S$
$S_n\{ {}_8^{17}\text{O}_9, {}_8^{18}\text{O}_{10} \}_+$	$(1d_{5/2})^2$	3.902
$\frac{1}{2}S_n\{ {}_8^{17}\text{O}_9, {}_8^{18}\text{O}_{10}, {}_8^{19}\text{O}_{11} \}_-$	$(1d_{5/2})^2$	3.996(1)
$\frac{1}{4}S_n\{ {}_8^{17}\text{O}_9, {}_8^{18}\text{O}_{10}, {}_8^{19}\text{O}_{11}, {}_8^{20}\text{O}_{12} \}_+$	$(1d_{5/2})^2$	3.934(2)
$S_n\{ {}_{20}^{41}\text{Ca}_{21}, {}_{20}^{42}\text{Ca}_{22} \}_+$	$(1f_{7/2})^2$	3.118
$\frac{1}{2}S_n\{ {}_{20}^{41}\text{Ca}_{21}, {}_{20}^{42}\text{Ca}_{22}, {}_{20}^{43}\text{Ca}_{23} \}_-$	$(1f_{7/2})^2$	3.333
$\frac{1}{2}S_n\{ {}_{20}^{41}\text{Ca}_{21}, {}_{20}^{42}\text{Ca}_{22}, {}_{20}^{43}\text{Ca}_{23}, {}_{20}^{44}\text{Ca}_{24} \}_-$	$(1f_{7/2})^2$	3.353
$S_n\{ {}_{82}^{209}\text{Pb}_{127}, {}_{82}^{210}\text{Pb}_{128} \}_+$	$(2g_{9/2})^2$	1.248(2)
$\frac{1}{2}S_n\{ {}_{82}^{209}\text{Pb}_{127}, {}_{82}^{210}\text{Pb}_{128}, {}_{82}^{211}\text{Pb}_{129} \}_-$	$(2g_{9/2})^2$	1.299(2)
$\frac{1}{4}S_n\{ {}_{82}^{209}\text{Pb}_{127}, {}_{82}^{210}\text{Pb}_{128}, {}_{82}^{211}\text{Pb}_{129}, {}_{82}^{212}\text{Pb}_{130} \}_+$	$(2g_{9/2})^2$	1.309(2)

Experimental evidence

P-wave pair binding in MeV

Nuclei	Predominant Orbitals	$2\Delta_p$
$S_n\{^{17}_8\text{O}_9(\frac{3}{2}^+), ^{18}_8\text{O}_{10}(1^+)\}_+$	$1d_{5/2} \otimes 1d_{3/2}$	0.172(12)
$\frac{1}{2}S_n\{^{55}_{26}\text{Fe}_{29}(\frac{5}{2}^-), ^{56}_{26}\text{Fe}_{30}(1^+), ^{57}_{26}\text{Fe}_{31}(\frac{5}{2}^-)\}_-$	$2p_{3/2} \otimes 1f_{5/2}$	0.139(3)
$\frac{1}{2}S_n\{^{57}_{28}\text{Ni}_{29}(\frac{5}{2}^-), ^{58}_{28}\text{Ni}_{30}(1^+), ^{59}_{28}\text{Ni}_{31}(\frac{5}{2}^-)\}_-$	$2p_{3/2} \otimes 1f_{5/2}$	0.245(1)

Experimental evidence

Quartet binding in MeV

Nuclei	Predominant Orbitals	$4\Delta_Q$
$S_{2n}\{^6\text{He}_4, ^8\text{He}_4\}_+$	$(1p_{3/2})^4$	1.150
$\frac{1}{2}S_{2n}\{^{18}_8\text{O}_{10}, ^{20}_8\text{O}_{12}, ^{22}_8\text{O}_{14}\}_-$	$(1d_{5/2})^4$	0.142(28)
$\frac{1}{2}S_{2n}\{^{42}_{20}\text{Ca}_{22}, ^{44}_{20}\text{Ca}_{24}, ^{46}_{20}\text{Ca}_{26}\}_-$	$(1f_{7/2})^4$	0.236(1)
$\frac{1}{2}S_{2n}\{^{44}_{20}\text{Ca}_{24}, ^{46}_{20}\text{Ca}_{26}, ^{48}_{20}\text{Ca}_{28}\}_+$	$(1f_{7/2})^4$	0.332(3)
$\frac{1}{2}S_{2n}\{^{106}_{50}\text{Sn}_{56}, ^{108}_{50}\text{Sn}_{58}, ^{110}_{50}\text{Sn}_{60}\}_+$	combination	0.033(11)
$\frac{1}{2}S_{2n}\{^{108}_{50}\text{Sn}_{58}, ^{110}_{50}\text{Sn}_{60}, ^{112}_{50}\text{Sn}_{62}\}_-$	combination	0.007(17)
$\frac{1}{2}S_{2n}\{^{110}_{50}\text{Sn}_{60}, ^{112}_{50}\text{Sn}_{62}, ^{114}_{50}\text{Sn}_{64}\}_+$	combination	0.025(16)
$\frac{1}{2}S_{2n}\{^{112}_{50}\text{Sn}_{62}, ^{114}_{50}\text{Sn}_{64}, ^{116}_{50}\text{Sn}_{66}\}_-$	combination	0.015(7)
$\frac{1}{2}S_{2n}\{^{114}_{50}\text{Sn}_{64}, ^{116}_{50}\text{Sn}_{66}, ^{118}_{50}\text{Sn}_{68}\}_+$	combination	0.050(30)
$\frac{1}{2}S_{2n}\{^{194}_{82}\text{Pb}_{112}, ^{196}_{82}\text{Pb}_{114}, ^{198}_{82}\text{Pb}_{116}\}_+$	combination	0.047(22)
$\frac{1}{2}S_{2n}\{^{196}_{82}\text{Pb}_{114}, ^{198}_{82}\text{Pb}_{116}, ^{200}_{82}\text{Pb}_{118}\}_-$	combination	0.057(16)
$\frac{1}{2}S_{2n}\{^{198}_{82}\text{Pb}_{116}, ^{200}_{82}\text{Pb}_{118}, ^{202}_{82}\text{Pb}_{120}\}_+$	combination	0.021(15)
$\frac{1}{2}S_{2n}\{^{200}_{82}\text{Pb}_{118}, ^{202}_{82}\text{Pb}_{120}, ^{204}_{82}\text{Pb}_{122}\}_-$	combination	0.013(13)
$\frac{1}{2}S_{2n}\{^{202}_{82}\text{Pb}_{120}, ^{204}_{82}\text{Pb}_{122}, ^{206}_{82}\text{Pb}_{124}\}_+$	combination	0.014(7)
$\frac{1}{2}S_{2n}\{^{204}_{82}\text{Pb}_{122}, ^{206}_{82}\text{Pb}_{124}, ^{208}_{82}\text{Pb}_{126}\}_-$	combination	0.110(2)
$\frac{1}{2}S_{2n}\{^{210}_{82}\text{Pb}_{128}, ^{212}_{82}\text{Pb}_{130}, ^{214}_{82}\text{Pb}_{132}\}_-$	$(2g_{9/2})^4$	0.014(2)
$\frac{1}{2}S_{2n}\{^{212}_{84}\text{Po}_{128}, ^{214}_{84}\text{Po}_{130}, ^{216}_{84}\text{Po}_{132}\}_-$	$(2g_{9/2})^4$	0.019(1)
$\frac{1}{2}S_{2n}\{^{214}_{84}\text{Po}_{130}, ^{216}_{84}\text{Po}_{132}, ^{218}_{84}\text{Po}_{134}\}_+$	$(2g_{9/2})^4$	0.015(2)
$\frac{1}{2}S_{2n}\{^{214}_{86}\text{Rn}_{128}, ^{216}_{86}\text{Rn}_{130}, ^{218}_{86}\text{Rn}_{132}\}_-$	$(2g_{9/2})^4$	0.079(12)

Summary and outlook

Using nuclear lattice effective field theory, we presented evidence for a new phase of matter called multimodal superfluidity exhibits simultaneous S-wave, P-wave, and quartet condensation. We showed that this phase emerges in neutron matter with realistic interactions and is a general feature of two-component Fermi systems with attractive s-wave and p-wave interactions. We discussed experimental evidence for multimodal superfluidity in nuclei and its implications for neutron star crust cooling and glitch dynamics.